

Numerical Methods for Hamiltonian Systems: Chaos Detection

Haris Skokos

**Department of Mathematics and Applied Mathematics
University of Cape Town, Cape Town, South Africa**

E-mail: haris.skokos@uct.ac.za

URL: <http://www.mth.uct.ac.za/~hskokos/>

This research has been co-financed by the European Union (European Social Fund – ESF) and Greek national funds through the Operational Program "Education and Lifelong Learning" of the National Strategic Reference Framework (NSRF) - Research Funding Program: Thales. Investing in knowledge society through the European Social Fund.

Outline

- **Hamiltonian systems – Symplectic maps**
 - ✓ **Variational equations**
 - ✓ **Poincaré Surface of Section**
 - ✓ **Lyapunov exponents**
- **Smaller ALignment Index – SALI**
 - ✓ **Definition**
 - ✓ **Behavior for chaotic and regular motion**
 - ✓ **Applications**
- **Generalized ALignment Index – GALI**
 - ✓ **Definition - Relation to SALI**
 - ✓ **Behavior for chaotic and regular motion**
 - ✓ **Applications**
 - ✓ **Global dynamics**
 - ✓ **Motion on low-dimensional tori**
- **Efficient integration of variational equations**
 - ✓ **Symplectic integrators**
 - ✓ **The tangent map (TM) method**
- **Conclusions**

Autonomous Hamiltonian systems

Consider an **N degree of freedom** autonomous Hamiltonian system having a Hamiltonian function of the form:

$$H(\overbrace{q_1, q_2, \dots, q_N}^{\text{positions}}, \overbrace{p_1, p_2, \dots, p_N}^{\text{momenta}})$$

The time evolution of an orbit (trajectory) with initial condition

$$P(0) = (q_1(0), q_2(0), \dots, q_N(0), p_1(0), p_2(0), \dots, p_N(0))$$

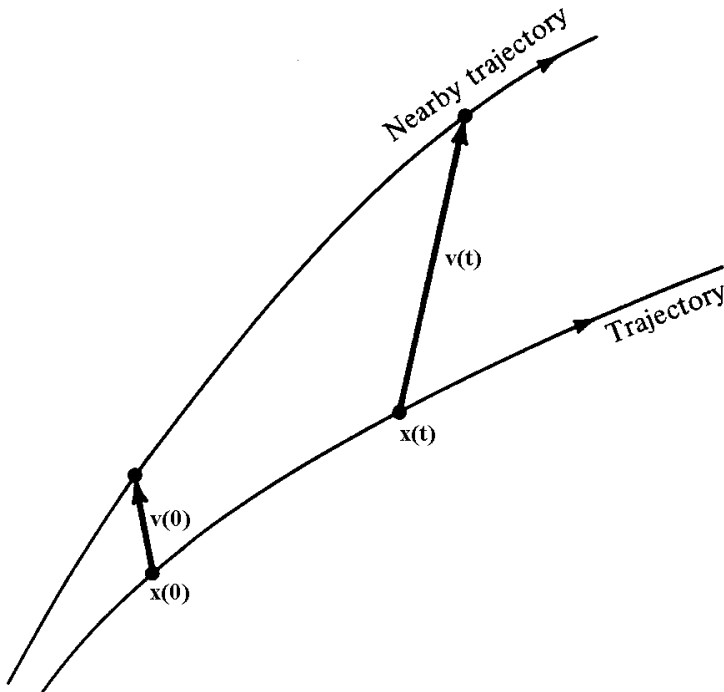
is governed by the **Hamilton's equations of motion**

$$\frac{dp_i}{dt} = -\frac{\partial H}{\partial q_i}, \quad \frac{dq_i}{dt} = \frac{\partial H}{\partial p_i}$$

Variational Equations

We use the notation $\mathbf{x} = (q_1, q_2, \dots, q_N, p_1, p_2, \dots, p_N)^T$. The **deviation vector** from a given orbit is denoted by

$$\mathbf{v} = (\delta x_1, \delta x_2, \dots, \delta x_n)^T, \text{ with } n=2N$$



The time evolution of \mathbf{v} is given by the so-called **variational equations**:

$$\frac{d\mathbf{v}}{dt} = -\mathbf{J} \cdot \mathbf{P} \cdot \mathbf{v}$$

where

$$\mathbf{J} = \begin{pmatrix} \mathbf{0}_N & -\mathbf{I}_N \\ \mathbf{I}_N & \mathbf{0}_N \end{pmatrix}, \quad \mathbf{P}_{ij} = \frac{\partial^2 \mathbf{H}}{\partial \mathbf{x}_i \partial \mathbf{x}_j} \quad i, j = 1, 2, \dots, n$$

Example (Hénon-Heiles system)

$$H = \frac{1}{2}(p_x^2 + p_y^2) + \frac{1}{2}(x^2 + y^2) + x^2y - \frac{1}{3}y^3$$

Hamilton's equations of motion:

$$\frac{dp_i}{dt} = -\frac{\partial H}{\partial q_i}, \quad \frac{dq_i}{dt} = \frac{\partial H}{\partial p_i} \Rightarrow \begin{cases} \dot{x} = p_x \\ \dot{y} = p_y \\ \dot{p}_x = -x - 2xy \\ \dot{p}_y = -y - x^2 + y^2 \end{cases}$$

In order to get the variational equations we **linearize** the above equations by substituting x, y, p_x, p_y with $x+v_1, y+v_2, p_x+v_3, p_y+v_4$ where $v=(v_1, v_2, v_3, v_4)$ is the deviation vector. So we get:

$$\begin{aligned} \dot{p}_x + \dot{v}_3 &= -x - v_1 - 2(x + v_1)(y + v_2) \Rightarrow \\ \cancel{\dot{p}_x} + \dot{v}_3 &= \cancel{-x - v_1 - 2xy} - 2xv_2 - 2yv_1 - \cancel{2v_1v_2} \Rightarrow \\ \dot{v}_3 &= -v_1 - 2yv_1 - 2xv_2 \end{aligned}$$

Example (Hénon-Heiles system)

Variational equations: $\frac{dv}{dt} = -\mathbf{J} \cdot \mathbf{P} \cdot \mathbf{v}$

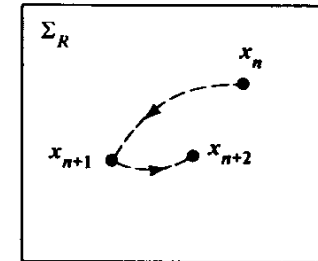
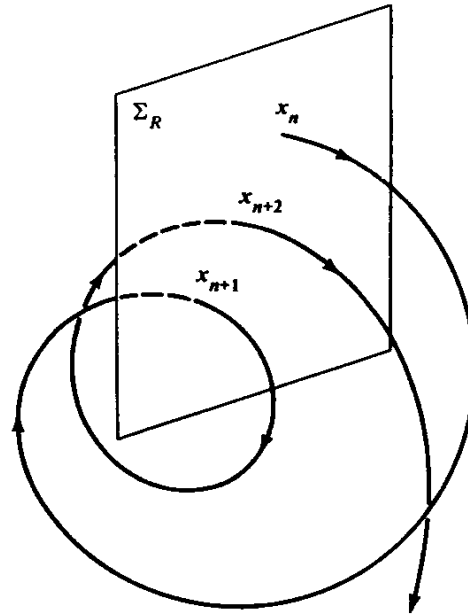
$$\begin{pmatrix} \dot{v}_1 \\ \dot{v}_2 \\ \dot{v}_3 \\ \dot{v}_4 \end{pmatrix} = - \begin{pmatrix} 0 & 0 & -1 & 0 \\ 0 & 0 & 0 & -1 \\ 1 & 0 & 0 & 0 \\ 0 & 1 & 0 & 0 \end{pmatrix} \begin{pmatrix} 1+2y & 2x & 0 & 0 \\ 2x & 1-2y & 0 & 0 \\ 0 & 0 & 1 & 0 \\ 0 & 0 & 0 & 1 \end{pmatrix} \begin{pmatrix} v_1 \\ v_2 \\ v_3 \\ v_4 \end{pmatrix}$$

$\dot{v}_1 = v_3$	+	$\dot{x} = p_x$
$\dot{v}_2 = v_4$		$\dot{y} = p_y$
$\dot{v}_3 = -v_1 - 2xv_2 - 2yv_1$		$\dot{p}_x = -x - 2xy$
$\dot{v}_4 = -v_2 - 2xv_1 + 2yv_2$		$\dot{p}_y = -y - x^2 + y^2$

Complete set of equations

Poincaré Surface of Section (PSS)

We can constrain the study of an $N+1$ degree of freedom Hamiltonian system to a **2N-dimensional subspace of the general phase space.**

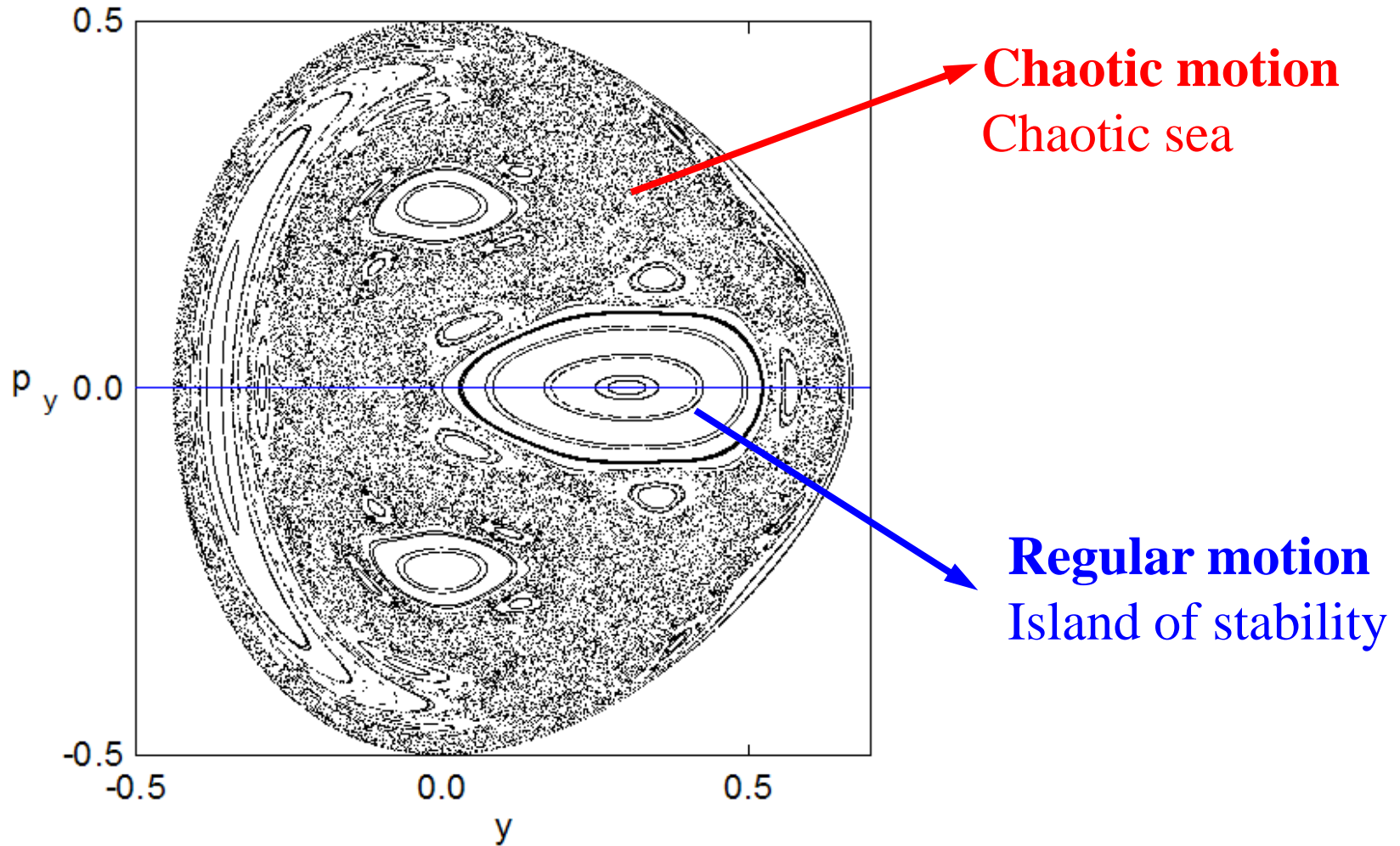


Lieberman & Lichtenberg, 1992, *Regular and Chaotic Dynamics*, Springer.

In general we can assume a PSS of the form $q_{N+1} = \text{constant}$. Then only variables $q_1, q_2, \dots, q_N, p_1, p_2, \dots, p_N$ are needed to describe the evolution of an orbit on the PSS, since p_{N+1} can be found from the Hamiltonian.

In this sense **an $N+1$ degree of freedom Hamiltonian system corresponds to a 2N-dimensional symplectic map.**

Hénon-Heiles system: PSS



Symplectic Maps

Consider an **2N-dimensional symplectic map T**. In this case we have **discrete time**.

This is an area-preserving map whose Jacobian matrix

$$\mathbf{M} = \frac{\partial \mathbf{T}}{\partial \mathbf{x}} = \begin{bmatrix} \frac{\partial \mathbf{T}_1}{\partial \mathbf{x}_1} & \frac{\partial \mathbf{T}_1}{\partial \mathbf{x}_2} & \dots & \frac{\partial \mathbf{T}_1}{\partial \mathbf{x}_{2N}} \\ \frac{\partial \mathbf{T}_2}{\partial \mathbf{x}_1} & \frac{\partial \mathbf{T}_2}{\partial \mathbf{x}_2} & \dots & \frac{\partial \mathbf{T}_2}{\partial \mathbf{x}_{2N}} \\ \vdots & \vdots & & \vdots \\ \frac{\partial \mathbf{T}_{2N}}{\partial \mathbf{x}_1} & \frac{\partial \mathbf{T}_{2N}}{\partial \mathbf{x}_2} & \dots & \frac{\partial \mathbf{T}_{2N}}{\partial \mathbf{x}_{2N}} \end{bmatrix}$$

satisfies

$$\mathbf{M}^T \cdot \mathbf{J}_{2N} \cdot \mathbf{M} = \mathbf{J}_{2N}$$

Symplectic Maps

The evolution of an **orbit** with initial condition

$$\mathbf{P}(0) = (\mathbf{x}_1(0), \mathbf{x}_2(0), \dots, \mathbf{x}_{2N}(0))$$

is governed by the **equations of map T**

$$\mathbf{P}(i+1) = \mathbf{T} \mathbf{P}(i) \quad , \quad i=0,1,2,\dots$$

The evolution of an initial **deviation vector**

$$\mathbf{v}(0) = (\delta\mathbf{x}_1(0), \delta\mathbf{x}_2(0), \dots, \delta\mathbf{x}_{2N}(0))$$

is given by the corresponding **tangent map**

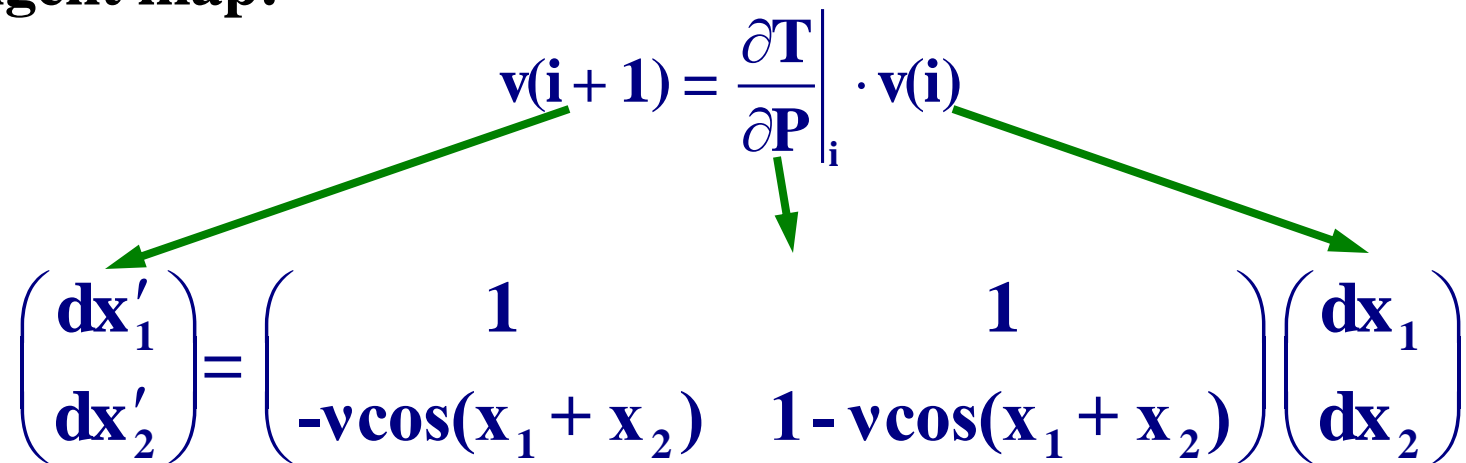
$$\mathbf{v}(i+1) = \left. \frac{\partial \mathbf{T}}{\partial \mathbf{P}} \right|_i \cdot \mathbf{v}(i) \quad , \quad i = 0, 1, 2, \dots$$

Example – 2D map

Equations of the map:

$$\begin{pmatrix} \mathbf{x}'_1 \\ \mathbf{x}'_2 \end{pmatrix} = \mathbf{T} \begin{pmatrix} \mathbf{x}_1 \\ \mathbf{x}_2 \end{pmatrix} \Rightarrow \begin{aligned} \mathbf{x}'_1 &= \mathbf{x}_1 + \mathbf{x}_2 \\ \mathbf{x}'_2 &= \mathbf{x}_2 - v \sin(\mathbf{x}_1 + \mathbf{x}_2) \end{aligned} \quad (\text{mod } 2\pi)$$

Tangent map:

$$\mathbf{v}(\mathbf{i} + 1) = \left. \frac{\partial \mathbf{T}}{\partial \mathbf{P}} \right|_{\mathbf{i}} \cdot \mathbf{v}(\mathbf{i})$$

$$\begin{pmatrix} d\mathbf{x}'_1 \\ d\mathbf{x}'_2 \end{pmatrix} = \begin{pmatrix} 1 & 1 \\ -v \cos(\mathbf{x}_1 + \mathbf{x}_2) & 1 - v \cos(\mathbf{x}_1 + \mathbf{x}_2) \end{pmatrix} \begin{pmatrix} d\mathbf{x}_1 \\ d\mathbf{x}_2 \end{pmatrix}$$

Lyapunov Exponents

Roughly speaking, the Lyapunov exponents of a given orbit characterize the **mean exponential rate of divergence** of trajectories surrounding it.

Consider an orbit in the $2N$ -dimensional phase space with **initial condition $\mathbf{x}(0)$** and an **initial deviation vector from it $\mathbf{v}(0)$** . Then the mean exponential rate of divergence is:

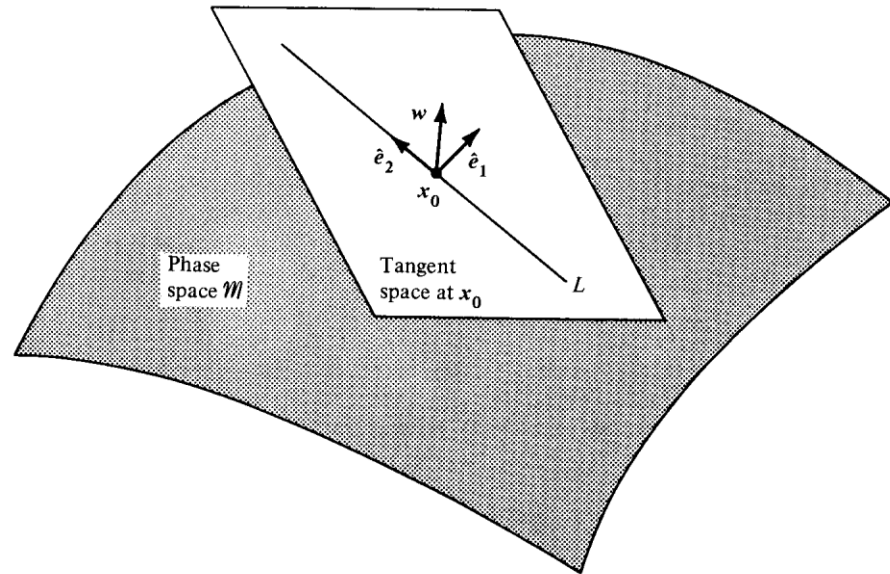
$$\sigma(\mathbf{x}(0), \mathbf{v}(0)) = \lim_{t \rightarrow \infty} \frac{1}{t} \ln \frac{\|\mathbf{v}(t)\|}{\|\mathbf{v}(0)\|}$$

Lyapunov Exponents

There exists an **M-dimensional basis** $\{\hat{e}_i\}$ of v such that for any v , σ takes one of the M (possibly nondistinct) values

$$\sigma_i(x(0)) = \sigma(x(0), \hat{e}_i)$$

which are the **Lyapunov exponents**.



Benettin & Galgani, 1979, in Laval and Gressillon (eds.), op cit, 93

In autonomous Hamiltonian systems the M exponents are ordered in **pairs of opposite sign numbers and two of them are 0**.

Computation of the Maximal Lyapunov Exponent

Due to the exponential growth of $v(t)$ (and of $d(t)=\|v(t)\|$) we **renormalize $v(t)$** from time to time.

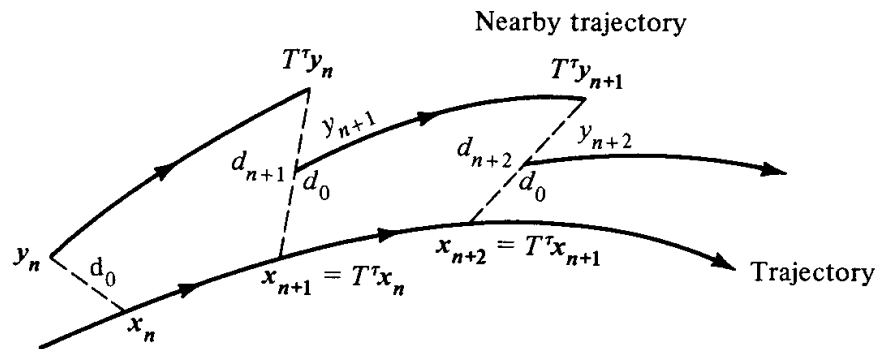


Figure 5.6. Numerical calculation of the maximal Liapunov characteristic exponent. Here $y = x + v$ and τ is a finite interval of time (after Benettin *et al.*, 1976).

Then the Maximal Lyapunov exponent is computed as

$$\sigma_1 = \lim_{n \rightarrow \infty} \frac{1}{n\tau} \sum_{i=1}^n \ln d_i$$

Maximum Lyapunov Exponent

$\sigma_1=0 \rightarrow$ Regular motion
 $\sigma_1 \neq 0 \rightarrow$ Chaotic motion

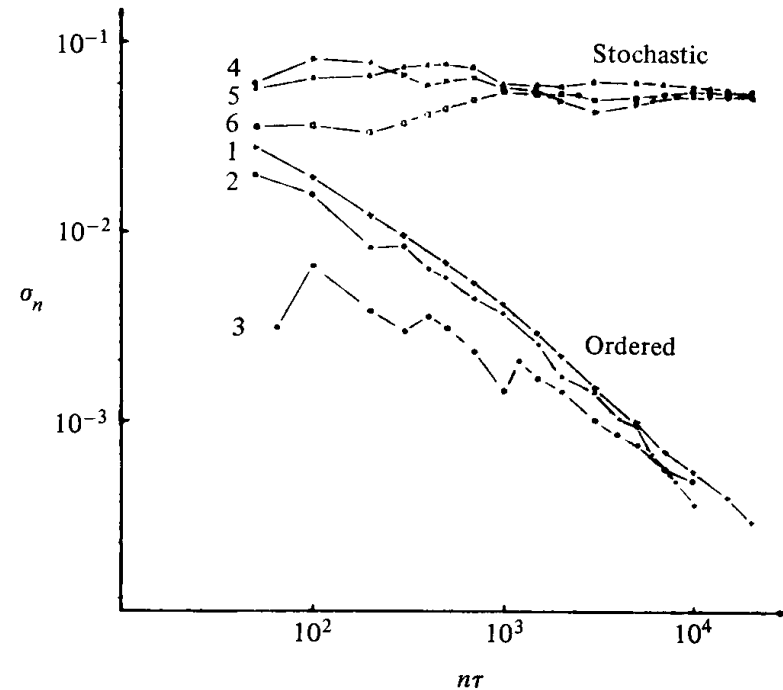


Figure 5.7. Behavior of σ_n at the intermediate energy $E = 0.125$ for initial points taken in the ordered (curves 1–3) or stochastic (curves 4–6) regions (after Benettin *et al.*, 1976).

If we start with more than one linearly independent deviation vectors they will **align to the direction defined by the largest Lyapunov exponent** for chaotic orbits.

**The
Smaller ALignment Index
(SALI)
method**

Definition of Smaller Alignment Index (SALI)

Consider the $2N$ -dimensional phase space of a conservative dynamical system (**symplectic map or Hamiltonian flow**).

An orbit in that space with initial condition :

$$P(0) = (x_1(0), x_2(0), \dots, x_{2N}(0))$$

and a deviation vector

$$v(0) = (\delta x_1(0), \delta x_2(0), \dots, \delta x_{2N}(0))$$

The evolution in time (in maps the time is discrete and is equal to the number n of the iterations) of a deviation vector is defined by:

- the **variational equations** (for Hamiltonian flows) and
- the equations of the **tangent map** (for mappings)

Definition of SALI

We follow the evolution in time of two different initial deviation vectors ($\mathbf{v}_1(\mathbf{0})$, $\mathbf{v}_2(\mathbf{0})$), and define SALI (**Ch.S. 2001, J. Phys. A**) as:

$$\text{SALI}(\mathbf{t}) = \min \left\{ \left\| \hat{\mathbf{v}}_1(\mathbf{t}) + \hat{\mathbf{v}}_2(\mathbf{t}) \right\|, \left\| \hat{\mathbf{v}}_1(\mathbf{t}) - \hat{\mathbf{v}}_2(\mathbf{t}) \right\| \right\}$$

where

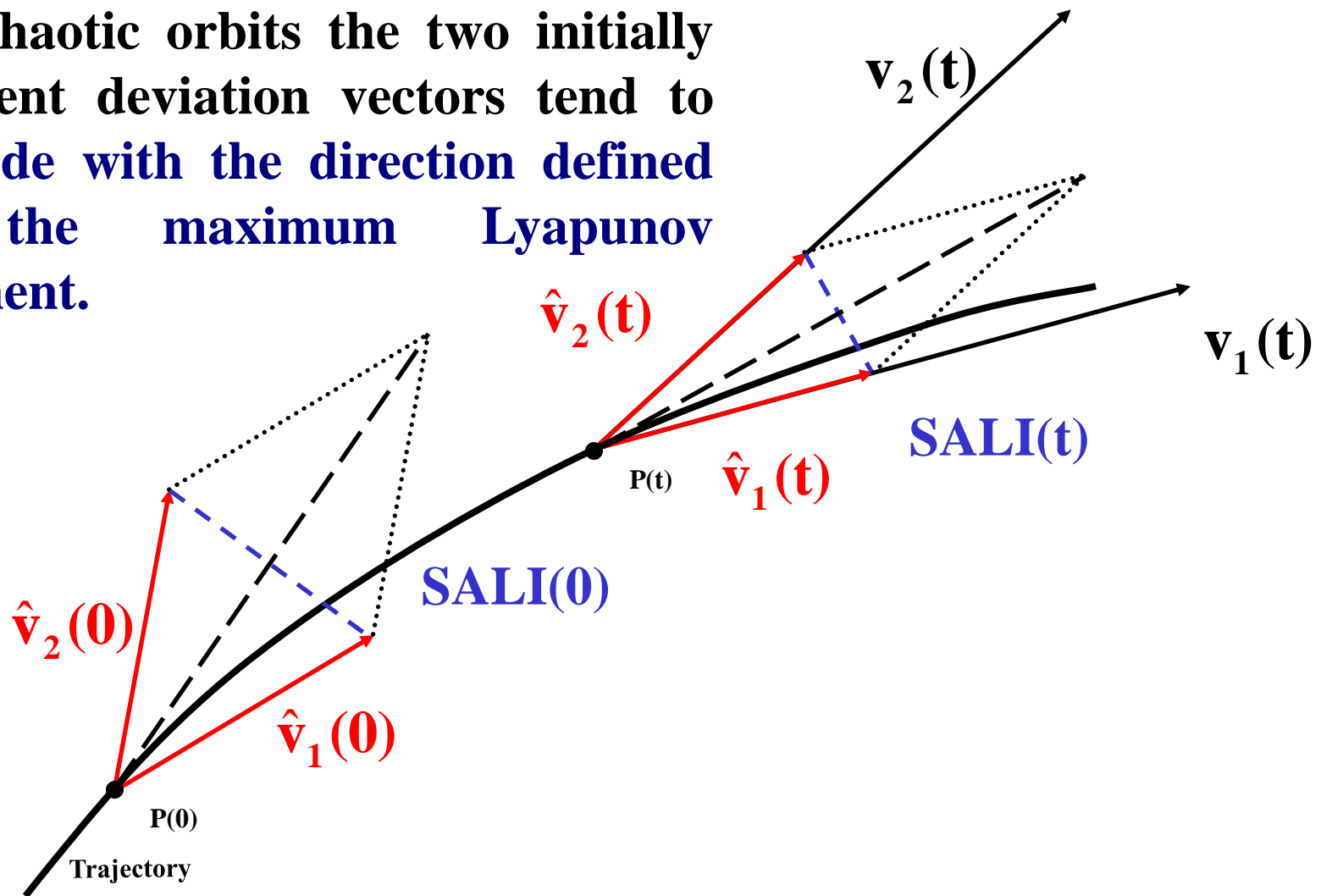
$$\hat{\mathbf{v}}_1(\mathbf{t}) = \frac{\mathbf{v}_1(\mathbf{t})}{\|\mathbf{v}_1(\mathbf{t})\|}$$

When the two vectors become **collinear**

$$\text{SALI}(\mathbf{t}) \rightarrow \mathbf{0}$$

Behavior of SALI for chaotic motion

For chaotic orbits the two initially different deviation vectors tend to coincide with the direction defined by the maximum Lyapunov exponent.



Behavior of SALI for chaotic motion

The evolution of a deviation vector can be approximated by:

$$\mathbf{v}_1(\mathbf{t}) = \sum_{i=1}^n \mathbf{c}_i^{(1)} e^{\sigma_i \mathbf{t}} \hat{\mathbf{u}}_i \approx \mathbf{c}_1^{(1)} e^{\sigma_1 \mathbf{t}} \hat{\mathbf{u}}_1 + \mathbf{c}_2^{(1)} e^{\sigma_2 \mathbf{t}} \hat{\mathbf{u}}_2$$

where $\sigma_1 > \sigma_2 \geq \dots \geq \sigma_n$ are the **Lyapunov exponents** and $\hat{\mathbf{u}}_j$ $j=1, 2, \dots, 2N$ the corresponding eigendirections.

In this approximation, we derive a leading order estimate of the ratio

$$\frac{\mathbf{v}_1(\mathbf{t})}{\|\mathbf{v}_1(\mathbf{t})\|} \approx \frac{\mathbf{c}_1^{(1)} e^{\sigma_1 \mathbf{t}} \hat{\mathbf{u}}_1 + \mathbf{c}_2^{(1)} e^{\sigma_2 \mathbf{t}} \hat{\mathbf{u}}_2}{|\mathbf{c}_1^{(1)}| e^{\sigma_1 \mathbf{t}}} = \pm \hat{\mathbf{u}}_1 + \frac{\mathbf{c}_2^{(1)}}{|\mathbf{c}_1^{(1)}|} e^{-(\sigma_1 - \sigma_2) \mathbf{t}} \hat{\mathbf{u}}_2$$

and an analogous expression for \mathbf{v}_2

$$\frac{\mathbf{v}_2(\mathbf{t})}{\|\mathbf{v}_2(\mathbf{t})\|} \approx \frac{\mathbf{c}_1^{(2)} e^{\sigma_1 \mathbf{t}} \hat{\mathbf{u}}_1 + \mathbf{c}_2^{(2)} e^{\sigma_2 \mathbf{t}} \hat{\mathbf{u}}_2}{|\mathbf{c}_1^{(2)}| e^{\sigma_1 \mathbf{t}}} = \pm \hat{\mathbf{u}}_1 + \frac{\mathbf{c}_2^{(2)}}{|\mathbf{c}_1^{(2)}|} e^{-(\sigma_1 - \sigma_2) \mathbf{t}} \hat{\mathbf{u}}_2$$

So we get:

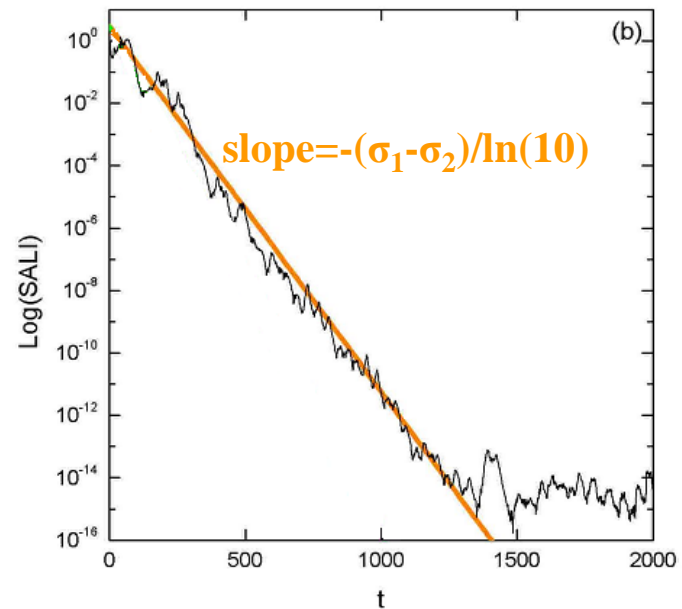
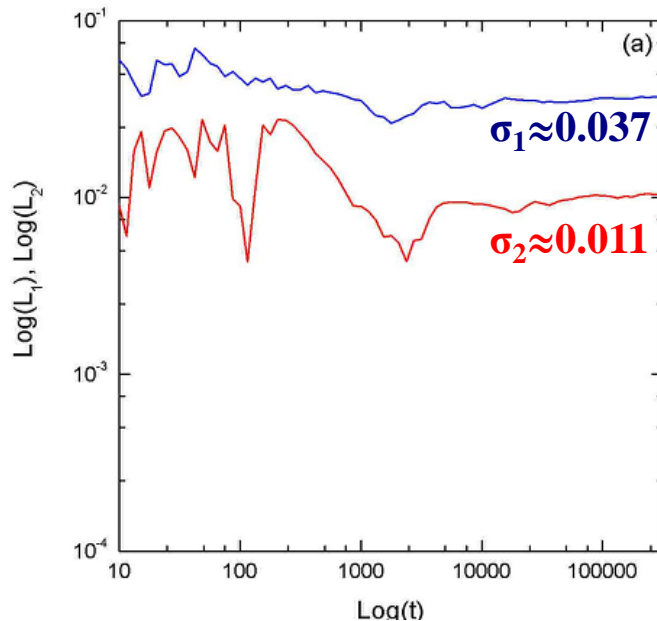
$$\text{SALI}(\mathbf{t}) = \min \left\{ \left\| \frac{\mathbf{v}_1(\mathbf{t})}{\|\mathbf{v}_1(\mathbf{t})\|} + \frac{\mathbf{v}_2(\mathbf{t})}{\|\mathbf{v}_2(\mathbf{t})\|} \right\|, \left\| \frac{\mathbf{v}_1(\mathbf{t})}{\|\mathbf{v}_1(\mathbf{t})\|} - \frac{\mathbf{v}_2(\mathbf{t})}{\|\mathbf{v}_2(\mathbf{t})\|} \right\| \right\} \approx \left| \frac{\mathbf{c}_2^{(1)}}{|\mathbf{c}_1^{(1)}|} \pm \frac{\mathbf{c}_2^{(2)}}{|\mathbf{c}_1^{(2)}|} \right| e^{-(\sigma_1 - \sigma_2) \mathbf{t}}$$

Behavior of SALI for chaotic motion

We test the validity of the approximation $\text{SALI} \propto e^{-(\sigma_1 - \sigma_2)t}$ (Ch.S., Antonopoulos, Bountis, Vrahatis, 2004, J. Phys. A) for a chaotic orbit of the 3D Hamiltonian

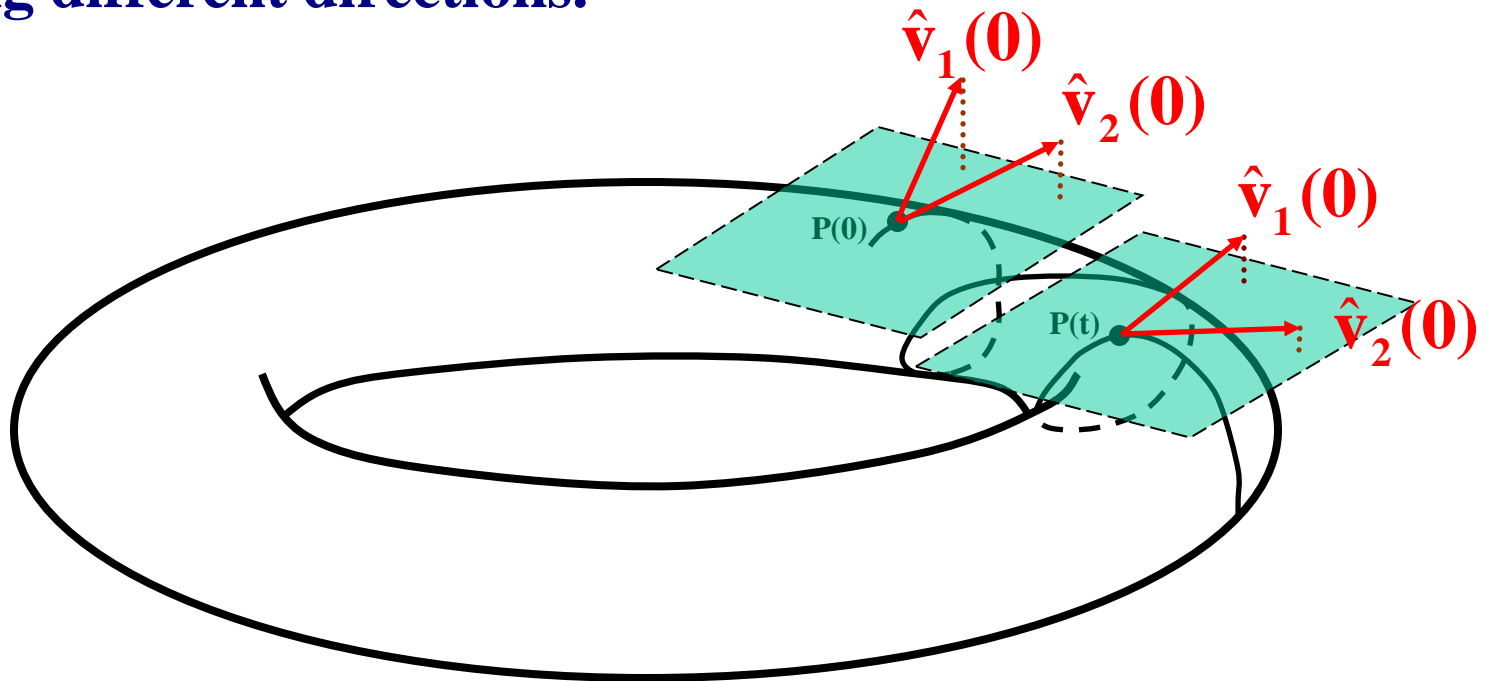
$$H = \sum_{i=1}^3 \frac{\omega_i}{2} (q_i^2 + p_i^2) + q_1^2 q_2 + q_1^2 q_3$$

with $\omega_1=1$, $\omega_2=1.4142$, $\omega_3=1.7321$, $H=0.09$



Behavior of SALI for regular motion

Regular motion occurs on a torus and two different initial deviation vectors become tangent to the torus, generally having different directions.



Applications – Hénon-Heiles system

As an example, we consider the 2D Hénon-Heiles system:

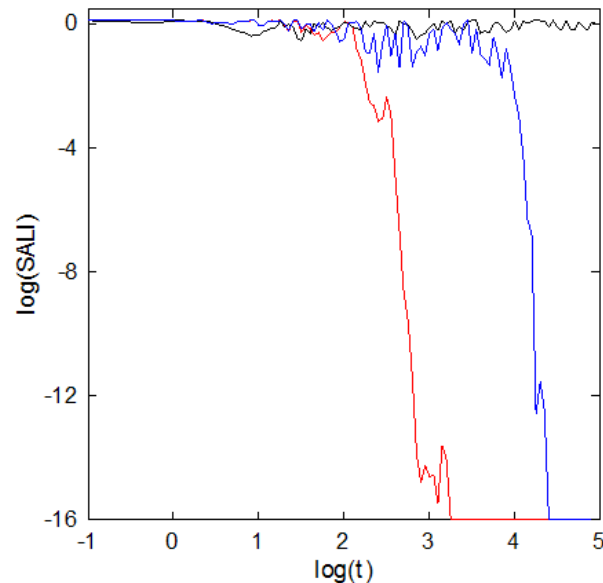
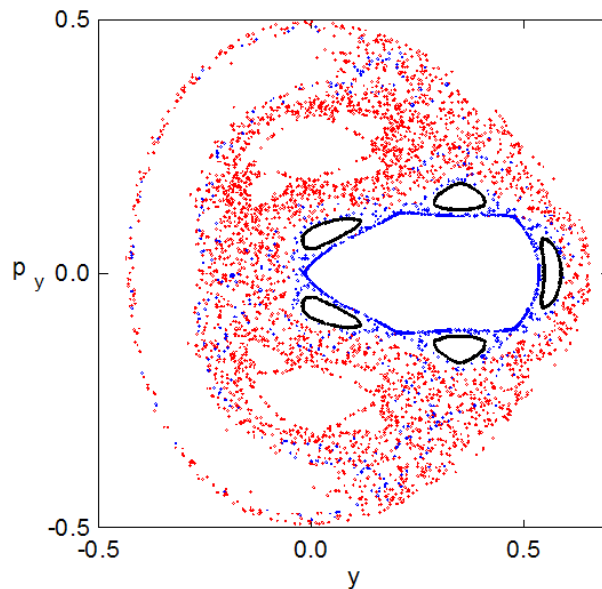
$$H_2 = \frac{1}{2}(p_x^2 + p_y^2) + \frac{1}{2}(x^2 + y^2) + x^2y - \frac{1}{3}y^3$$

For $E=1/8$ we consider the orbits with initial conditions:

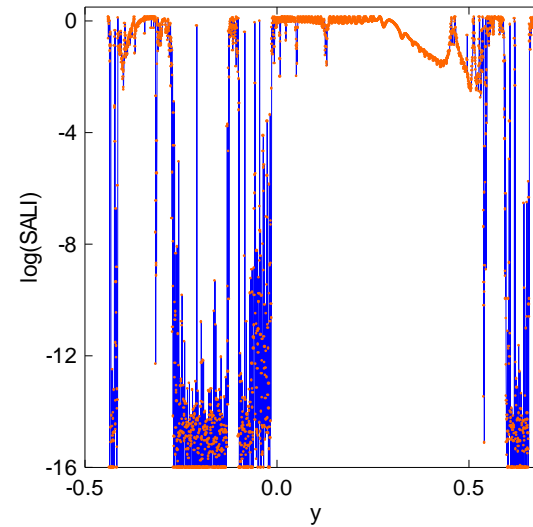
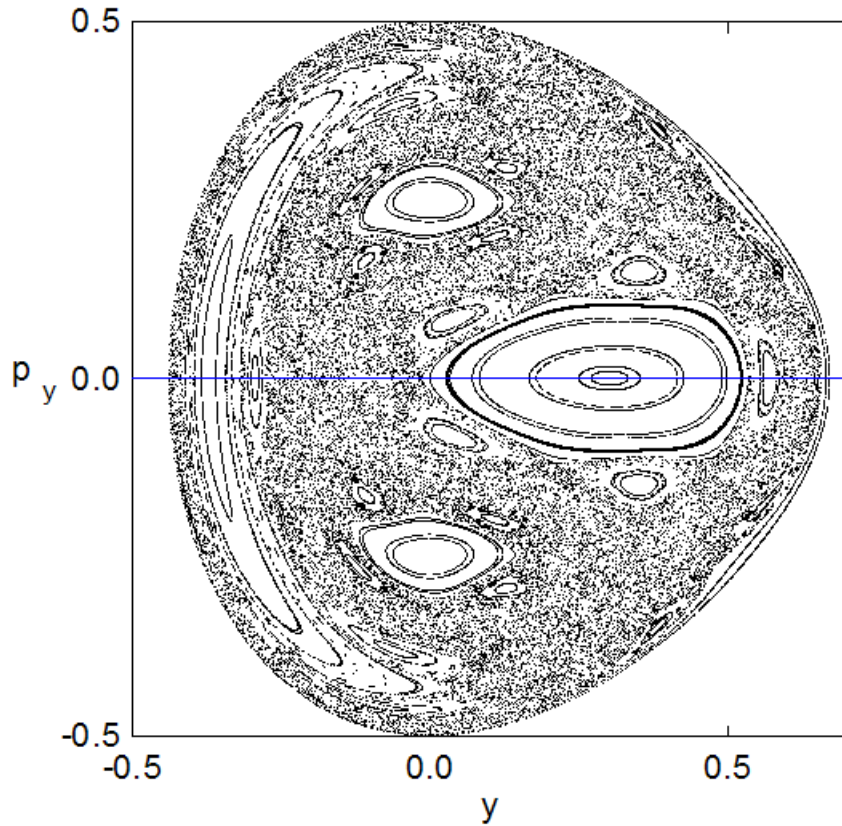
Regular orbit, $x=0$, $y=0.55$, $p_x=0.2417$, $p_y=0$

Chaotic orbit, $x=0$, $y=-0.016$, $p_x=0.49974$, $p_y=0$

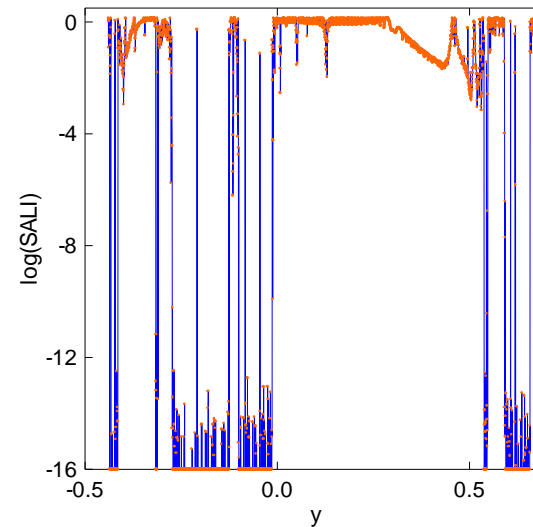
Chaotic orbit, $x=0$, $y=-0.01344$, $p_x=0.49982$, $p_y=0$



Applications – Hénon-Heiles system

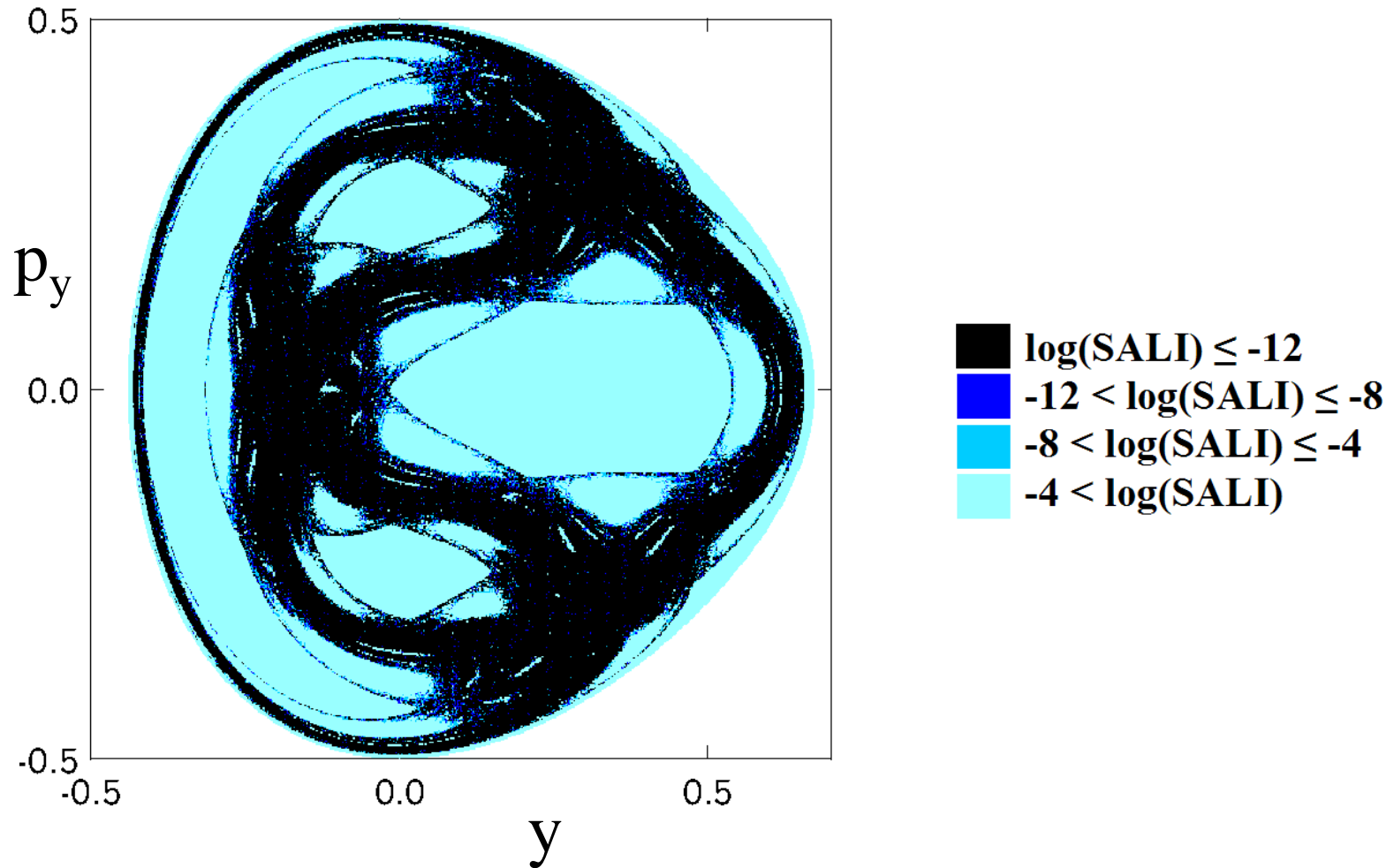


$t=1000$



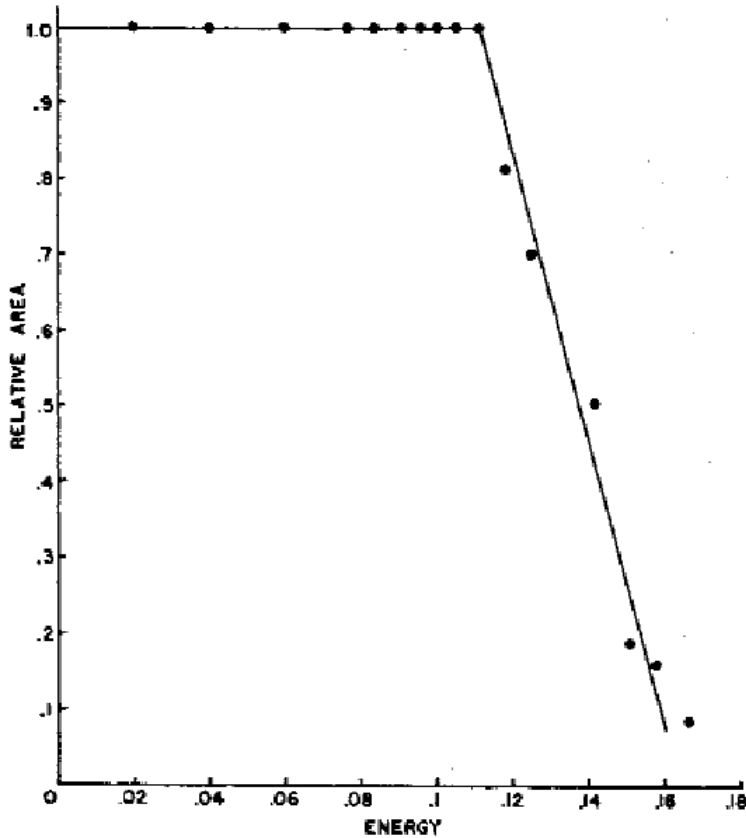
$t=4000$

Applications – Hénon-Heiles system

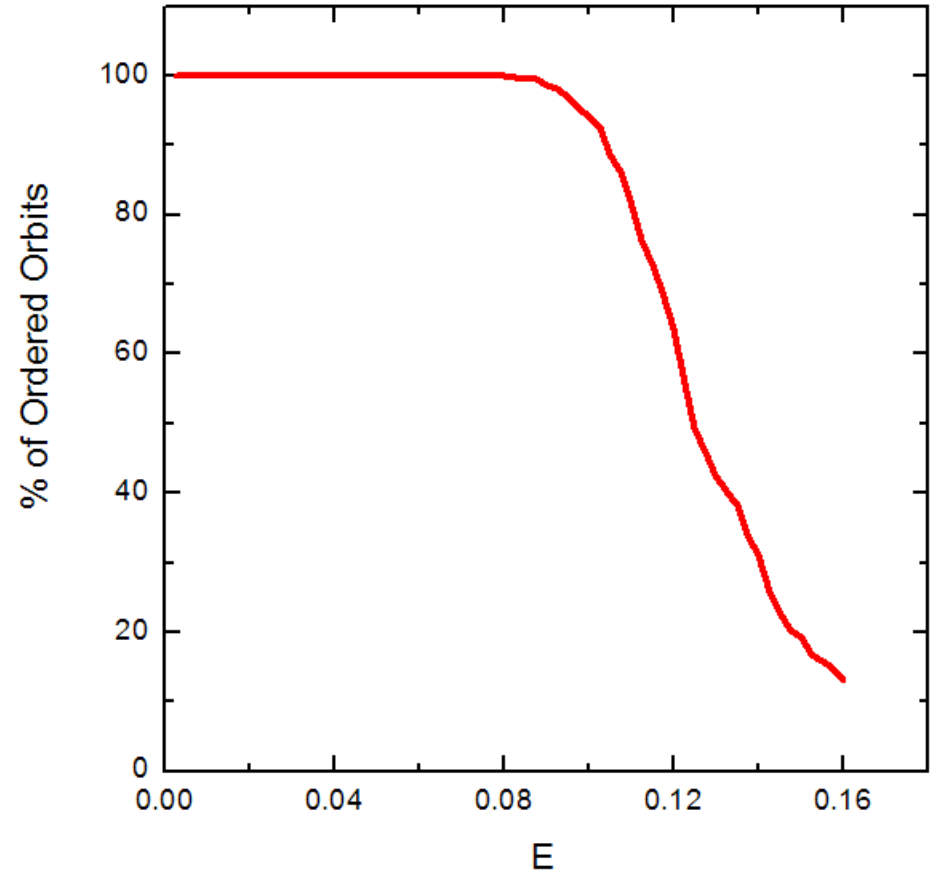


Applications – Hénon-Heiles system

The percentage of non chaotic orbits ($SALI > 10^{-8}$ for $t=1000$)



Hénon-Heiles (1964) Astron. J. 69, 73.



A. Manos (2004) Master Thesis, Univ. of Patras

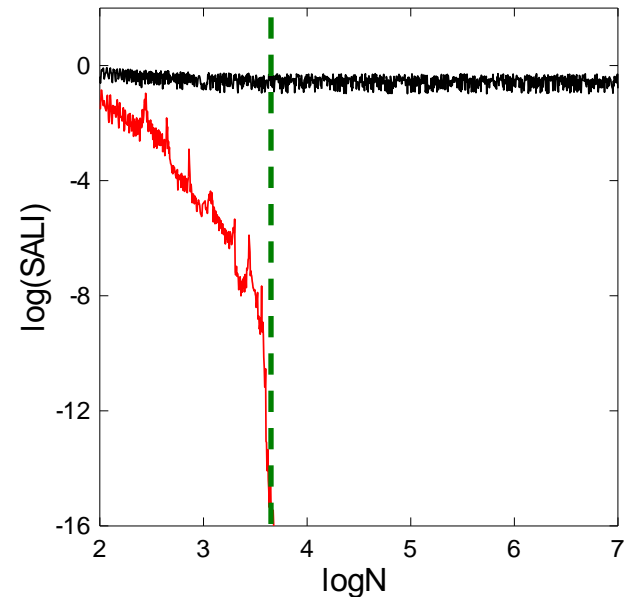
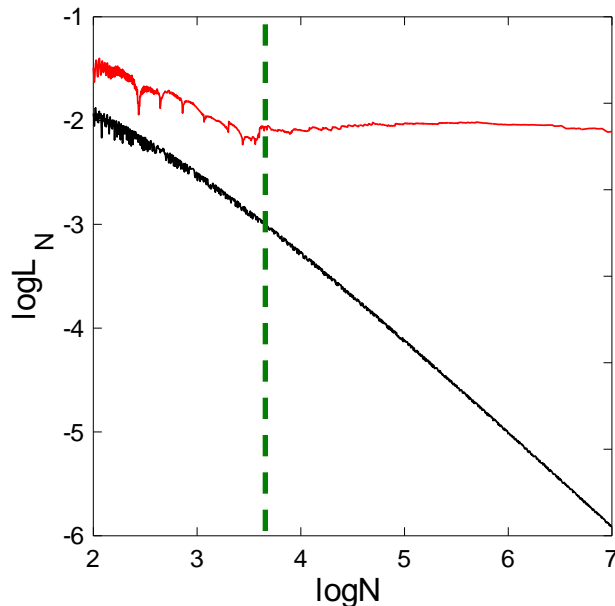
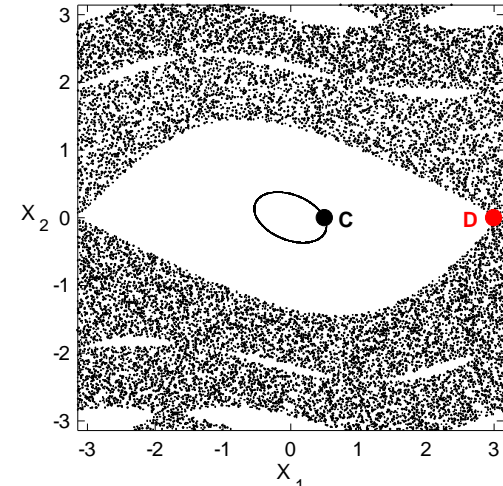
Applications – 4D map

$$\begin{aligned}
 \mathbf{x}'_1 &= \mathbf{x}_1 + \mathbf{x}_2 \\
 \mathbf{x}'_2 &= \mathbf{x}_2 - \nu \sin(\mathbf{x}_1 + \mathbf{x}_2) - \mu [1 - \cos(\mathbf{x}_1 + \mathbf{x}_2 + \mathbf{x}_3 + \mathbf{x}_4)] \\
 \mathbf{x}'_3 &= \mathbf{x}_3 + \mathbf{x}_4 \\
 \mathbf{x}'_4 &= \mathbf{x}_4 - \kappa \sin(\mathbf{x}_3 + \mathbf{x}_4) - \mu [1 - \cos(\mathbf{x}_1 + \mathbf{x}_2 + \mathbf{x}_3 + \mathbf{x}_4)]
 \end{aligned} \pmod{2\pi}$$

For $\nu=0.5$, $\kappa=0.1$, $\mu=0.1$ we consider the orbits:

regular orbit C with initial conditions $x_1=0.5, x_2=0, x_3=0.5, x_4=0$.

chaotic orbit D with initial conditions $x_1=3, x_2=0, x_3=0.5, x_4=0$.



Applications – 4D Accelerator map

We consider the 4D symplectic map

$$\begin{pmatrix} x_1' \\ x_2' \\ x_3' \\ x_4' \end{pmatrix} = \begin{pmatrix} \cos\omega_1 & -\sin\omega_1 & 0 & 0 \\ \sin\omega_1 & \cos\omega_1 & 0 & 0 \\ 0 & 0 & \cos\omega_2 & -\sin\omega_2 \\ 0 & 0 & \sin\omega_2 & \cos\omega_2 \end{pmatrix} \times \begin{pmatrix} x_1 \\ x_2 + x_1^2 - x_3^2 \\ x_3 \\ x_4 - 2x_1x_3 \end{pmatrix}$$

describing the **instantaneous sextupole ‘kicks’** experienced by a particle as it passes through an accelerator (Turchetti & Scandale 1991, Bountis & Tompaidis 1991, Vrahatis et al. 1996, 1997).

x_1 and x_3 are the particle’s deflections from the ideal circular orbit, in the horizontal and vertical directions respectively.

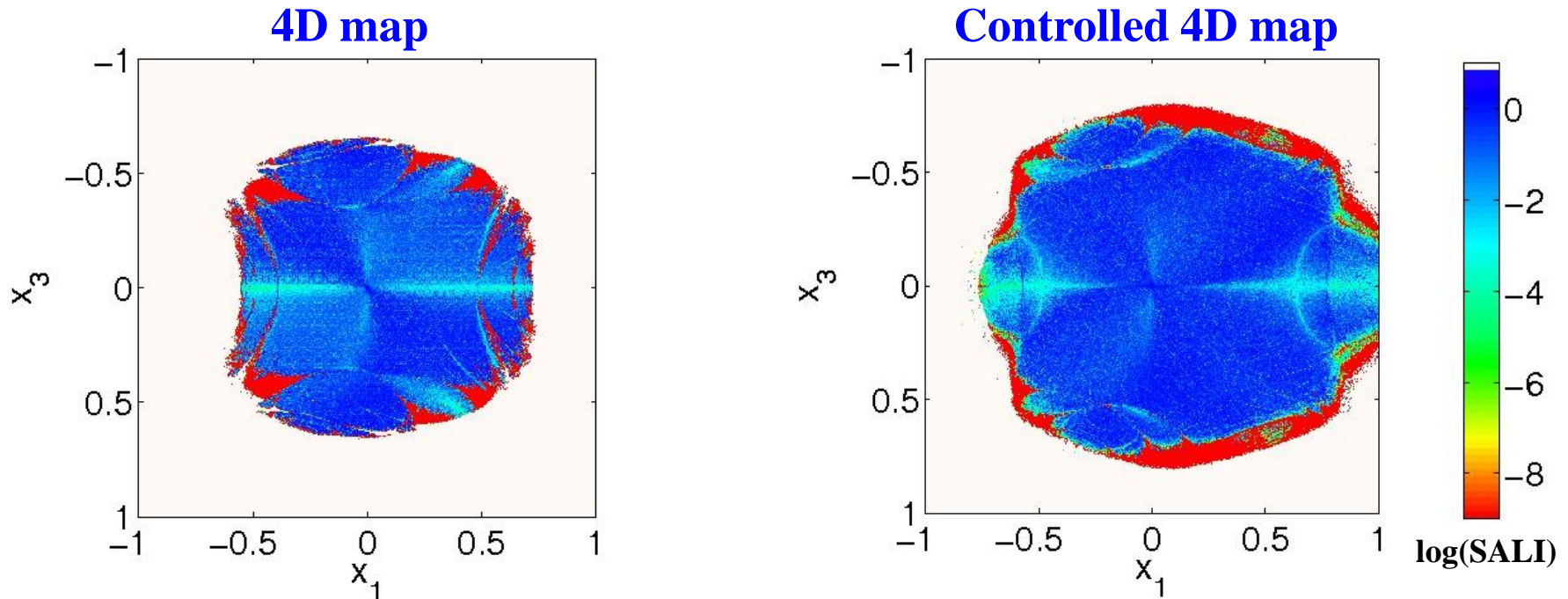
x_2 and x_4 are the associated momenta

ω_1, ω_2 are related to the accelerator’s tunes q_x, q_y by $\omega_1=2\pi q_x, \omega_2=2\pi q_y$

Our goal is to estimate the **region of stability** of the particle’s motion, the so-called **dynamic aperture** of the beam (Bountis, Ch.S., 2006, Nucl. Inst Meth. Phys Res. A) and to increase its size using chaos control techniques (Boreaux, Carletti, Ch.S., Vittot, 2012, Commun. Nonlinear Sci. Num. Simulat. – Boreaux, Carletti, Ch.S., Papaphilippou, Vittot, 2012, Int. J. Bifur. Chaos).

4D Accelerator map – "Global" study

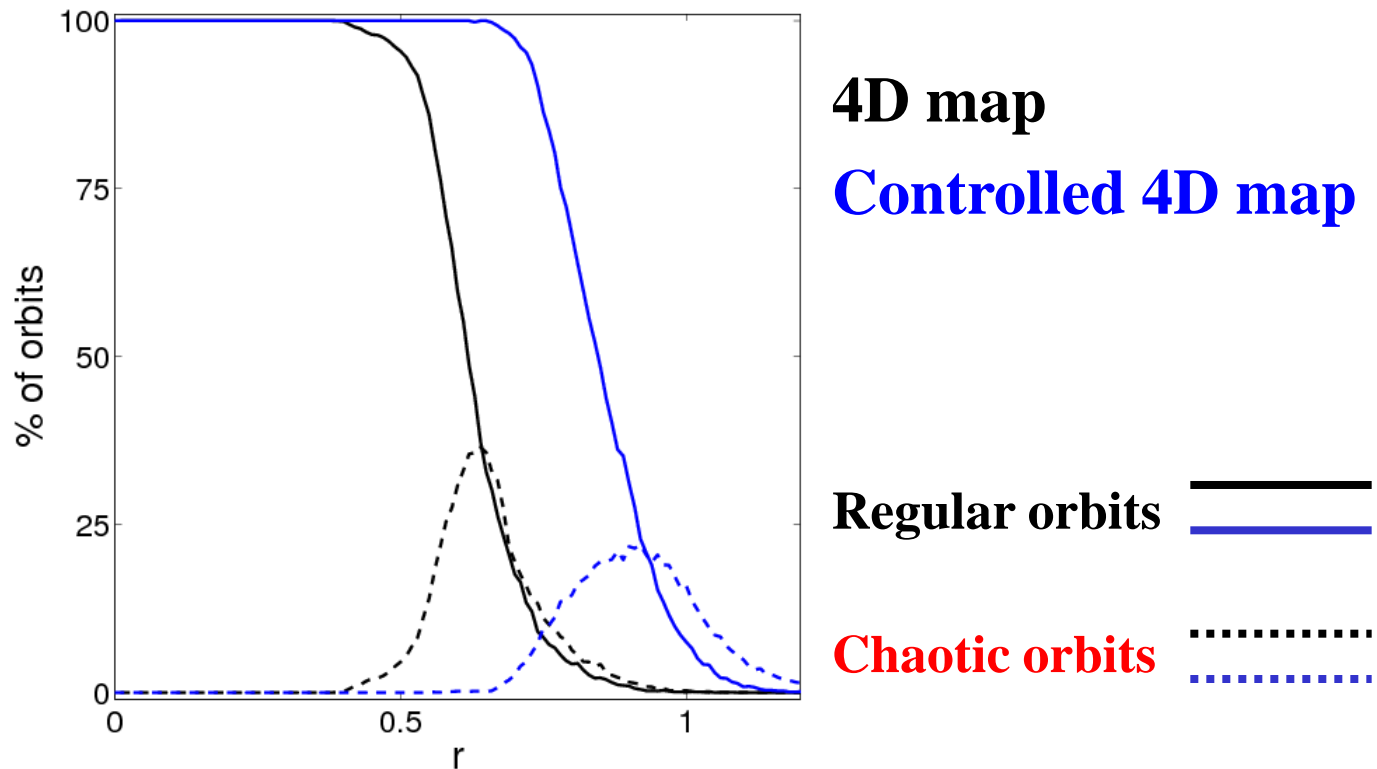
Regions of **different values of the SALI** on the subspace $x_2(0)=x_4(0)=0$, after 10^5 iterations ($q_x=0.61803$ $q_y=0.4152$)



4D Accelerator map – "Global" study

Increase of the dynamic aperture

We evolve many orbits in 4D hyperspheres of radius r centered at $x_1=x_2=x_3=x_4=0$, for 10^5 iterations.



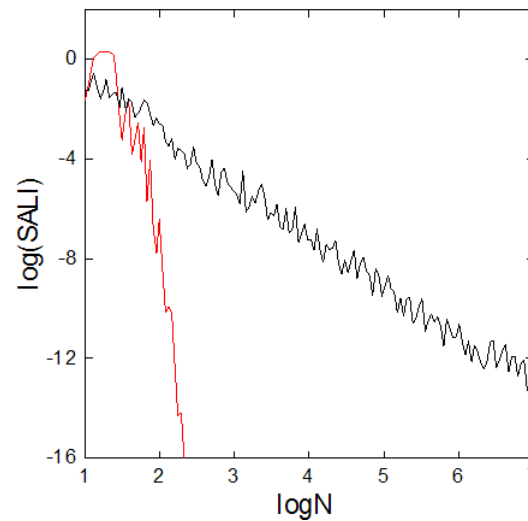
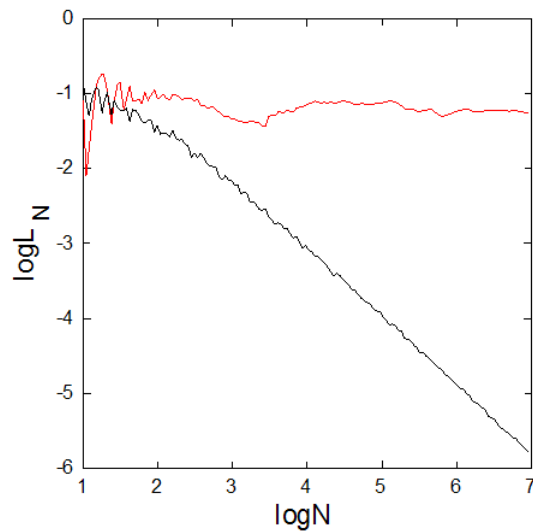
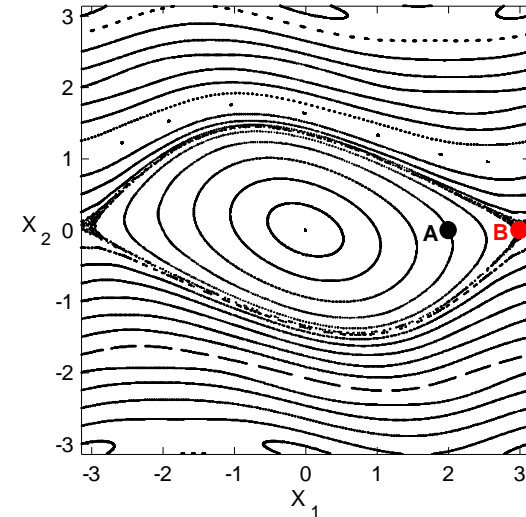
Applications – 2D map

$$\begin{aligned} \mathbf{x}'_1 &= \mathbf{x}_1 + \mathbf{x}_2 \\ \mathbf{x}'_2 &= \mathbf{x}_2 - \nu \sin(\mathbf{x}_1 + \mathbf{x}_2) \end{aligned} \quad (\text{mod } 2\pi)$$

For $\nu=0.5$ we consider the orbits:

regular orbit A with initial conditions $x_1=2, x_2=0$.

chaotic orbit B with initial conditions $x_1=3, x_2=0$.



Behavior of SALI

2D maps

SALI $\rightarrow 0$ both for regular and chaotic orbits

following, however, completely different time rates which allows us to distinguish between the two cases.

Hamiltonian flows and multidimensional maps

SALI $\rightarrow 0$ for chaotic orbits

SALI \rightarrow constant $\neq 0$ for regular orbits

Questions

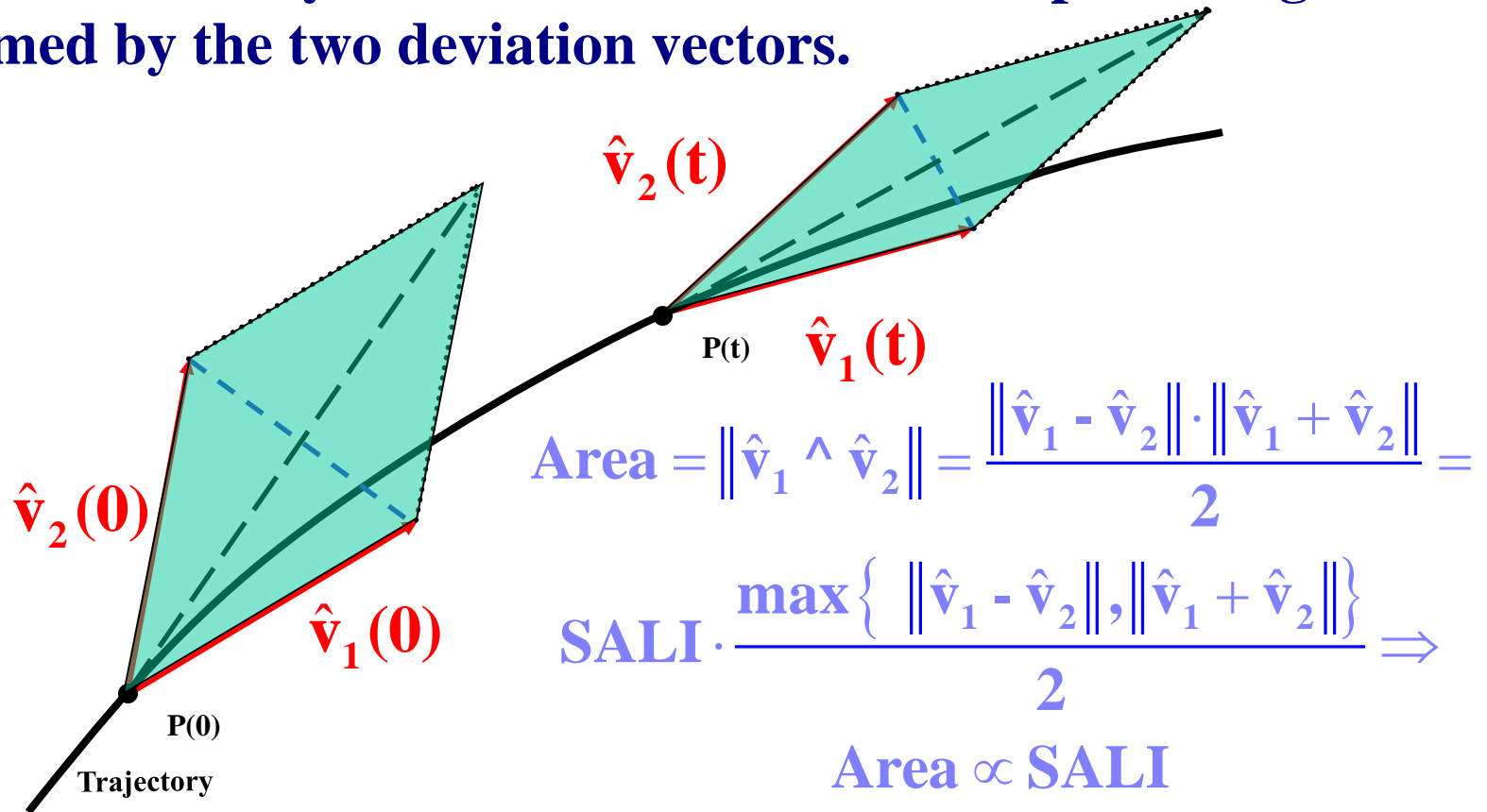
Can we generalize SALI so that the new index:

- **Can rapidly reveal the nature of chaotic orbits with $\sigma_1 \approx \sigma_2$ ($\text{SALI} \propto e^{-(\sigma_1 - \sigma_2)t}$)?**
- **Depends on several Lyapunov exponents for chaotic orbits?**
- **Exhibits power-law decay for regular orbits depending on the dimensionality of the tangent space of the reference orbit as for 2D maps?**

**The
Generalized ALignment Indices
(GALIs)
method**

Definition of Generalized Alignment Index (GALI)

SALI effectively measures the 'area' of the parallelogram formed by the two deviation vectors.



Definition of GALI

In the case of an N degree of freedom Hamiltonian system or a $2N$ symplectic map we follow the evolution of

k deviation vectors with $2 \leq k \leq 2N$,

and define (Ch.S., Bountis, Antonopoulos, 2007, Physica D) the Generalized Alignment Index (GALI) of order k :

$$\text{GALI}_k(\mathbf{t}) = \left\| \hat{\mathbf{v}}_1(\mathbf{t}) \wedge \hat{\mathbf{v}}_2(\mathbf{t}) \wedge \dots \wedge \hat{\mathbf{v}}_k(\mathbf{t}) \right\|$$

where

$$\hat{\mathbf{v}}_1(\mathbf{t}) = \frac{\mathbf{v}_1(\mathbf{t})}{\|\mathbf{v}_1(\mathbf{t})\|}$$

Wedge product

We consider as a basis of the $2N$ -dimensional tangent space of the system the usual set of orthonormal vectors:

$$\hat{\mathbf{e}}_1 = (1, 0, 0, \dots, 0), \hat{\mathbf{e}}_2 = (0, 1, 0, \dots, 0), \dots, \hat{\mathbf{e}}_{2N} = (0, 0, 0, \dots, 1)$$

Then for k deviation vectors we have:

$$\begin{bmatrix} \hat{\mathbf{v}}_1 \\ \hat{\mathbf{v}}_2 \\ \vdots \\ \hat{\mathbf{v}}_k \end{bmatrix} = \begin{bmatrix} \mathbf{v}_{11} & \mathbf{v}_{12} & \cdots & \mathbf{v}_{12N} \\ \mathbf{v}_{21} & \mathbf{v}_{22} & \cdots & \mathbf{v}_{22N} \\ \vdots & \vdots & & \vdots \\ \mathbf{v}_{k1} & \mathbf{v}_{k2} & \cdots & \mathbf{v}_{k2N} \end{bmatrix} \cdot \begin{bmatrix} \hat{\mathbf{e}}_1 \\ \hat{\mathbf{e}}_2 \\ \vdots \\ \hat{\mathbf{e}}_{2N} \end{bmatrix}$$

$$\hat{\mathbf{v}}_1 \wedge \hat{\mathbf{v}}_2 \wedge \cdots \wedge \hat{\mathbf{v}}_k = \sum_{1 \leq i_1 < i_2 < \cdots < i_k \leq 2N} \begin{vmatrix} \mathbf{v}_{1i_1} & \mathbf{v}_{1i_2} & \cdots & \mathbf{v}_{1i_k} \\ \mathbf{v}_{2i_1} & \mathbf{v}_{2i_2} & \cdots & \mathbf{v}_{2i_k} \\ \vdots & \vdots & & \vdots \\ \mathbf{v}_{ki_1} & \mathbf{v}_{ki_2} & \cdots & \mathbf{v}_{ki_k} \end{vmatrix} \hat{\mathbf{e}}_{i_1} \wedge \hat{\mathbf{e}}_{i_2} \wedge \cdots \wedge \hat{\mathbf{e}}_{i_k}$$

Norm of wedge product

We define as ‘norm’ of the wedge product the quantity :

$$\|\hat{\mathbf{v}}_1 \wedge \hat{\mathbf{v}}_2 \wedge \cdots \wedge \hat{\mathbf{v}}_k\| = \left\{ \sum_{1 \leq i_1 < i_2 < \cdots < i_k \leq 2N} \begin{vmatrix} \mathbf{v}_{1i_1} & \mathbf{v}_{1i_2} & \cdots & \mathbf{v}_{1i_k} \\ \mathbf{v}_{2i_1} & \mathbf{v}_{2i_2} & \cdots & \mathbf{v}_{2i_k} \\ \vdots & \vdots & & \vdots \\ \mathbf{v}_{ki_1} & \mathbf{v}_{ki_2} & \cdots & \mathbf{v}_{ki_k} \end{vmatrix}^2 \right\}^{1/2}$$

Computation of GALI - Example

Let us compute GALI_3 in the case of 2D Hamiltonian system (4-dimensional phase space).

$$\begin{bmatrix} \hat{\mathbf{v}}_1 \\ \hat{\mathbf{v}}_2 \\ \hat{\mathbf{v}}_3 \end{bmatrix} = \begin{bmatrix} \mathbf{v}_{11} & \mathbf{v}_{12} & \mathbf{v}_{13} & \mathbf{v}_{14} \\ \mathbf{v}_{21} & \mathbf{v}_{22} & \mathbf{v}_{23} & \mathbf{v}_{24} \\ \mathbf{v}_{31} & \mathbf{v}_{32} & \mathbf{v}_{33} & \mathbf{v}_{34} \end{bmatrix} \cdot \begin{bmatrix} \hat{\mathbf{e}}_1 \\ \hat{\mathbf{e}}_2 \\ \hat{\mathbf{e}}_3 \\ \hat{\mathbf{e}}_4 \end{bmatrix}$$

$$\text{GALI}_3 = \|\hat{\mathbf{v}}_1 \wedge \hat{\mathbf{v}}_2 \wedge \hat{\mathbf{v}}_3\| = \left\{ \begin{array}{l} \text{Columns } \mathbf{1} \quad \mathbf{2} \quad \mathbf{3} \\ \left| \begin{array}{ccc} \mathbf{v}_{11} & \mathbf{v}_{12} & \mathbf{v}_{13} \\ \mathbf{v}_{21} & \mathbf{v}_{22} & \mathbf{v}_{23} \\ \mathbf{v}_{31} & \mathbf{v}_{32} & \mathbf{v}_{33} \end{array} \right|^2 + \left| \begin{array}{ccc} \mathbf{1} \quad \mathbf{2} \quad \mathbf{4} \\ \mathbf{v}_{11} & \mathbf{v}_{12} & \mathbf{v}_{14} \\ \mathbf{v}_{21} & \mathbf{v}_{22} & \mathbf{v}_{24} \\ \mathbf{v}_{31} & \mathbf{v}_{32} & \mathbf{v}_{34} \end{array} \right|^2 + \\ \left. \left| \begin{array}{ccc} \mathbf{1} \quad \mathbf{3} \quad \mathbf{4} \\ \mathbf{v}_{11} & \mathbf{v}_{13} & \mathbf{v}_{14} \\ \mathbf{v}_{21} & \mathbf{v}_{23} & \mathbf{v}_{24} \\ \mathbf{v}_{31} & \mathbf{v}_{33} & \mathbf{v}_{34} \end{array} \right|^2 + \left| \begin{array}{ccc} \mathbf{2} \quad \mathbf{3} \quad \mathbf{4} \\ \mathbf{v}_{12} & \mathbf{v}_{13} & \mathbf{v}_{14} \\ \mathbf{v}_{22} & \mathbf{v}_{23} & \mathbf{v}_{24} \\ \mathbf{v}_{32} & \mathbf{v}_{33} & \mathbf{v}_{34} \end{array} \right|^2 \right\}^{1/2}$$

Efficient computation of GALI

For k deviation vectors:

$$\begin{bmatrix} \hat{\mathbf{v}}_1 \\ \hat{\mathbf{v}}_2 \\ \vdots \\ \hat{\mathbf{v}}_k \end{bmatrix} = \begin{bmatrix} \mathbf{v}_{11} & \mathbf{v}_{12} & \cdots & \mathbf{v}_{12N} \\ \mathbf{v}_{21} & \mathbf{v}_{22} & \cdots & \mathbf{v}_{22N} \\ \vdots & \vdots & & \vdots \\ \mathbf{v}_{k1} & \mathbf{v}_{k2} & \cdots & \mathbf{v}_{k2N} \end{bmatrix} \cdot \begin{bmatrix} \hat{\mathbf{e}}_1 \\ \hat{\mathbf{e}}_2 \\ \vdots \\ \hat{\mathbf{e}}_{2N} \end{bmatrix} = \mathbf{A} \cdot \begin{bmatrix} \hat{\mathbf{e}}_1 \\ \hat{\mathbf{e}}_2 \\ \vdots \\ \hat{\mathbf{e}}_{2N} \end{bmatrix}$$

the 'norm' of the wedge product is given by:

$$\|\hat{\mathbf{v}}_1 \wedge \hat{\mathbf{v}}_2 \wedge \cdots \wedge \hat{\mathbf{v}}_k\| = \left\{ \sum_{1 \leq i_1 < i_2 < \cdots < i_k \leq 2N} \begin{vmatrix} \mathbf{v}_{1i_1} & \mathbf{v}_{1i_2} & \cdots & \mathbf{v}_{1i_k} \\ \mathbf{v}_{2i_1} & \mathbf{v}_{2i_2} & \cdots & \mathbf{v}_{2i_k} \\ \vdots & \vdots & & \vdots \\ \mathbf{v}_{ki_1} & \mathbf{v}_{ki_2} & \cdots & \mathbf{v}_{ki_k} \end{vmatrix}^2 \right\}^{1/2} = \sqrt{\det(\mathbf{A} \cdot \mathbf{A}^T)}$$

Efficient computation of GALI

From Singular Value Decomposition (SVD) of A^T we get:

$$A^T = U \cdot W \cdot V^T$$

where U is a column-orthogonal $2N \times k$ matrix ($U^T \cdot U = I$), V^T is a $k \times k$ orthogonal matrix ($V \cdot V^T = I$), and W is a diagonal $k \times k$ matrix with positive or zero elements, the so-called **singular values**. So, we get:

$$\det(A \cdot A^T) = \det(V \cdot W^T \cdot U^T \cdot U \cdot W \cdot V^T) = \det(V \cdot W \cdot I \cdot W \cdot V^T) =$$

$$\det(V \cdot W^2 \cdot V^T) = \det(V \cdot \text{diag}(w_1^2, w_2^2, \dots, w_k^2) \cdot V^T) = \prod_{i=1}^k w_i^2$$

Thus, GALI_k is computed by:

$$\text{GALI}_k = \sqrt{\det(A \cdot A^T)} = \prod_{i=1}^k w_i \Rightarrow \log(\text{GALI}_k) = \sum_{i=1}^k \log(w_i)$$

Behavior of $GALI_k$ for chaotic motion

$GALI_k$ ($2 \leq k \leq 2N$) tends exponentially to zero with exponents that involve the values of the first k largest Lyapunov exponents $\sigma_1, \sigma_2, \dots, \sigma_k$:

$$GALI_k(t) \propto e^{-[(\sigma_1 - \sigma_2) + (\sigma_1 - \sigma_3) + \dots + (\sigma_1 - \sigma_k)]t}$$

The above relation is valid even if some Lyapunov exponents are equal, or very close to each other.

Behavior of $GALI_k$ for chaotic motion

Using the approximation:

$$\mathbf{v}_i(t) = \sum_{j=1}^{2N} \mathbf{c}_j^i e^{\sigma_j t} \hat{\mathbf{u}}_j = \mathbf{c}_1^i e^{\sigma_1 t} \hat{\mathbf{u}}_1 + \mathbf{c}_2^i e^{\sigma_2 t} \hat{\mathbf{u}}_2 + \dots + \mathbf{c}_{2N}^i e^{\sigma_{2N} t} \hat{\mathbf{u}}_{2N}, \quad \|\mathbf{v}_i(t)\| \approx |\mathbf{c}_1^i| e^{\sigma_1 t}$$

where $\sigma_1 > \sigma_2 \geq \dots \geq \sigma_n$ are the **Lyapunov exponents**, and $\hat{\mathbf{u}}_j$ $j=1, 2, \dots, 2N$ the corresponding eigendirections, we get

$$\begin{bmatrix} \hat{\mathbf{v}}_1 \\ \hat{\mathbf{v}}_2 \\ \vdots \\ \hat{\mathbf{v}}_k \end{bmatrix} = \begin{bmatrix} s_1 & \frac{\mathbf{c}_2^1}{|\mathbf{c}_1^1|} e^{-(\sigma_1 - \sigma_2)t} & \frac{\mathbf{c}_3^1}{|\mathbf{c}_1^1|} e^{-(\sigma_1 - \sigma_3)t} & \dots & \frac{\mathbf{c}_{2N}^1}{|\mathbf{c}_1^1|} e^{-(\sigma_1 - \sigma_{2N})t} \\ s_2 & \frac{\mathbf{c}_2^2}{|\mathbf{c}_1^2|} e^{-(\sigma_1 - \sigma_2)t} & \frac{\mathbf{c}_3^2}{|\mathbf{c}_1^2|} e^{-(\sigma_1 - \sigma_3)t} & \dots & \frac{\mathbf{c}_{2N}^2}{|\mathbf{c}_1^2|} e^{-(\sigma_1 - \sigma_{2N})t} \\ \vdots & \vdots & \vdots & \vdots & \vdots \\ s_k & \frac{\mathbf{c}_2^k}{|\mathbf{c}_1^k|} e^{-(\sigma_1 - \sigma_2)t} & \frac{\mathbf{c}_3^k}{|\mathbf{c}_1^k|} e^{-(\sigma_1 - \sigma_3)t} & \dots & \frac{\mathbf{c}_{2N}^k}{|\mathbf{c}_1^k|} e^{-(\sigma_1 - \sigma_{2N})t} \end{bmatrix} \cdot \begin{bmatrix} \hat{\mathbf{u}}_1 \\ \hat{\mathbf{u}}_2 \\ \vdots \\ \hat{\mathbf{u}}_{2N} \end{bmatrix}$$

with $s_i = \text{sign}(\mathbf{c}_1^i)$.

Behavior of $GALI_k$ for chaotic motion

From all determinants appearing in the definition of $GALI_k$ the one that **decreases the slowest** is the one containing the first k columns of the previous matrix:

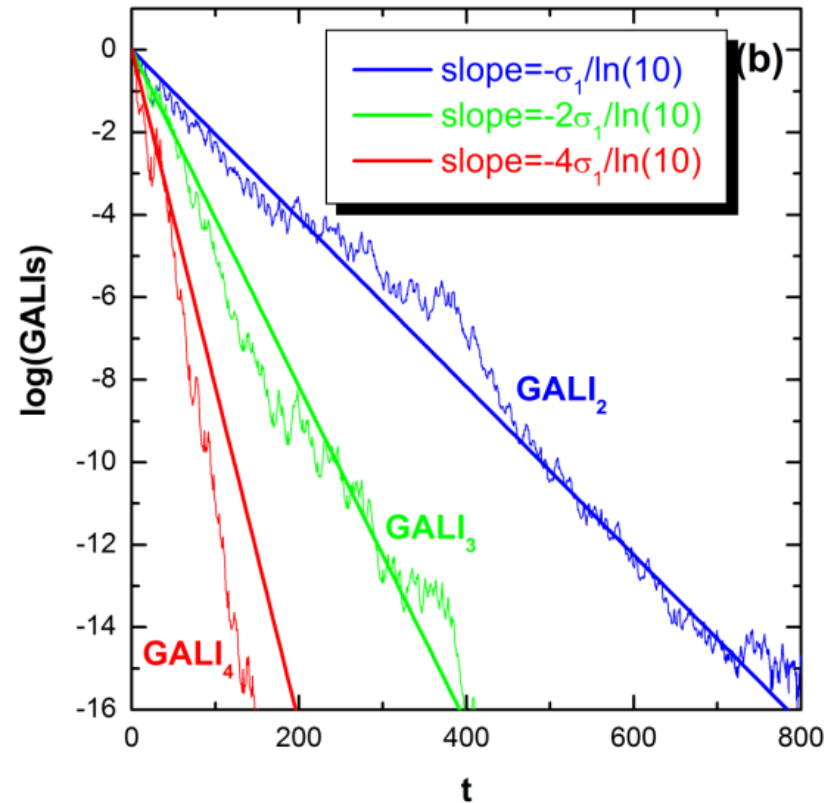
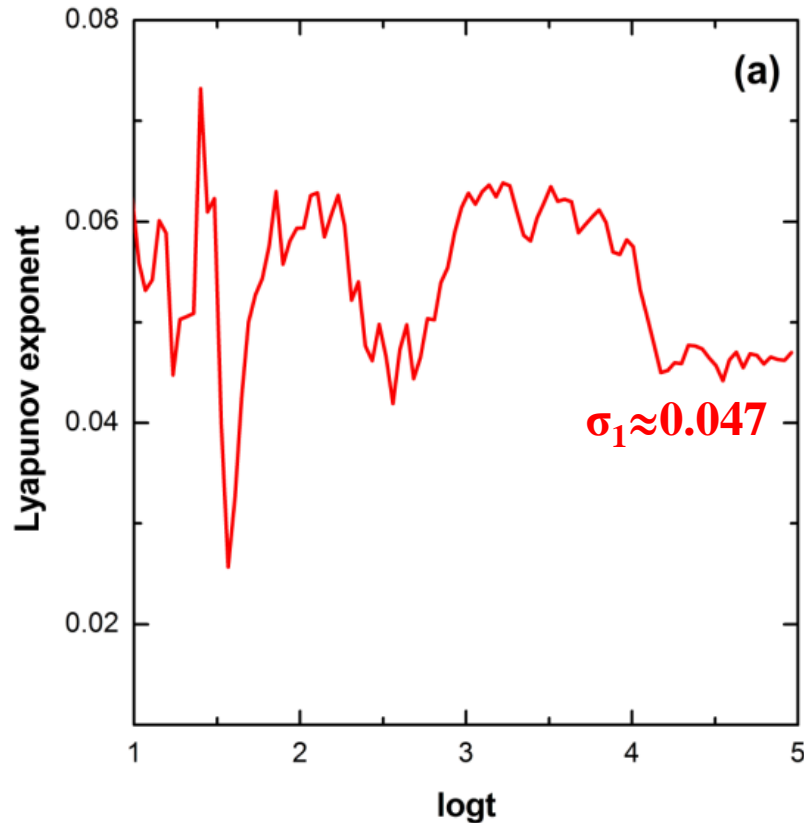
$$\begin{vmatrix}
 s_1 & \frac{c_2^1}{|c_1^1|} e^{-(\sigma_1 - \sigma_2)t} & \frac{c_3^1}{|c_1^1|} e^{-(\sigma_1 - \sigma_3)t} & \dots & \frac{c_k^1}{|c_1^1|} e^{-(\sigma_1 - \sigma_k)t} \\
 s_2 & \frac{c_2^2}{|c_1^2|} e^{-(\sigma_1 - \sigma_2)t} & \frac{c_3^2}{|c_1^2|} e^{-(\sigma_1 - \sigma_3)t} & \dots & \frac{c_k^2}{|c_1^2|} e^{-(\sigma_1 - \sigma_k)t} \\
 \vdots & \vdots & \vdots & \vdots & \vdots \\
 s_k & \frac{c_2^k}{|c_1^k|} e^{-(\sigma_1 - \sigma_2)t} & \frac{c_3^k}{|c_1^k|} e^{-(\sigma_1 - \sigma_3)t} & \dots & \frac{c_k^k}{|c_1^k|} e^{-(\sigma_1 - \sigma_k)t}
 \end{vmatrix}
 =
 \begin{vmatrix}
 s_1 & \frac{c_2^1}{|c_1^1|} & \frac{c_3^1}{|c_1^1|} & \dots & \frac{c_k^1}{|c_1^1|} \\
 s_2 & \frac{c_2^2}{|c_1^2|} & \frac{c_3^2}{|c_1^2|} & \dots & \frac{c_k^2}{|c_1^2|} \\
 \vdots & \vdots & \vdots & \vdots & \vdots \\
 s_k & \frac{c_2^k}{|c_1^k|} & \frac{c_3^k}{|c_1^k|} & \dots & \frac{c_k^k}{|c_1^k|}
 \end{vmatrix}
 \cdot e^{-[(\sigma_1 - \sigma_2) + (\sigma_1 - \sigma_3) + \dots + (\sigma_1 - \sigma_k)]t}$$

Thus

$$GALI_k(t) \propto e^{-[(\sigma_1 - \sigma_2) + (\sigma_1 - \sigma_3) + \dots + (\sigma_1 - \sigma_k)]t}$$

Behavior of $GALI_k$ for chaotic motion

2D Hamiltonian (Hénon-Heiles system)

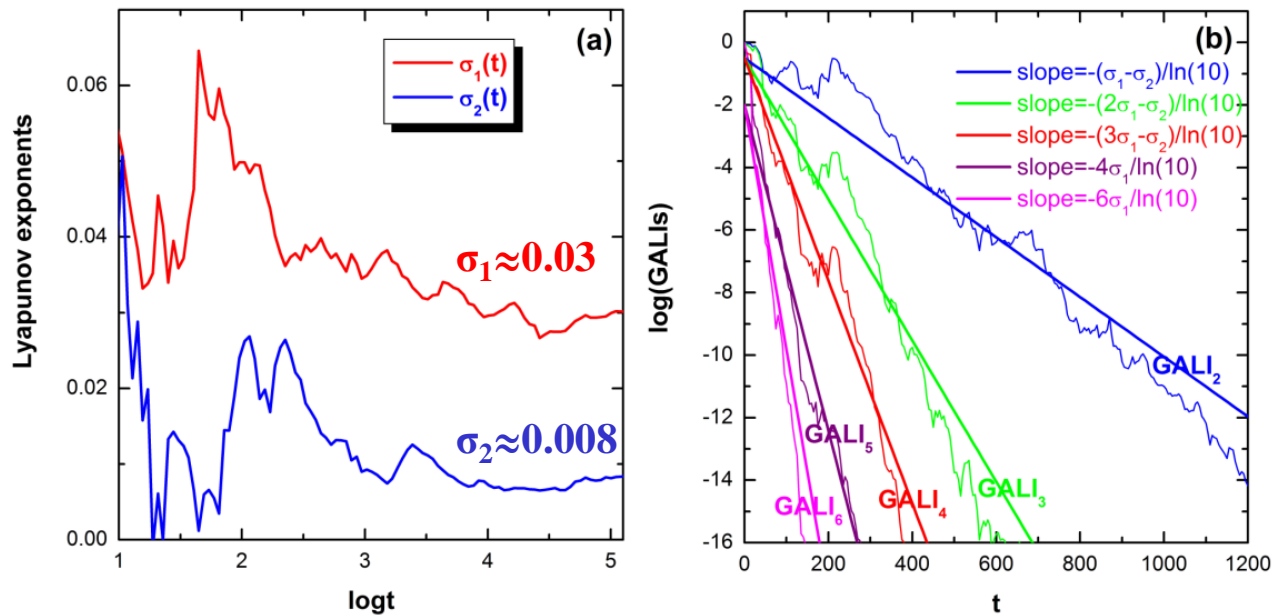


Behavior of $GALI_k$ for chaotic motion

3D system:

$$H_3 = \sum_{i=1}^3 \frac{\omega_i}{2} (q_i^2 + p_i^2) + q_1^2 q_2 + q_1^2 q_3$$

with $\omega_1=1$, $\omega_2=\sqrt{2}$, $\omega_3=\sqrt{3}$, $H_3=0.09$.

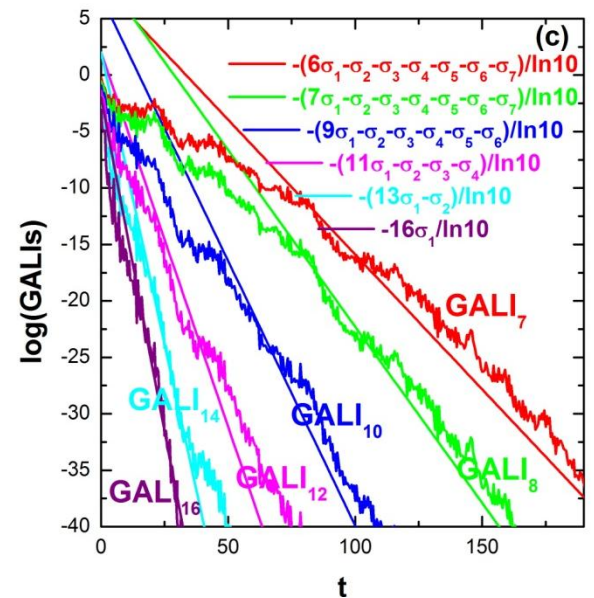
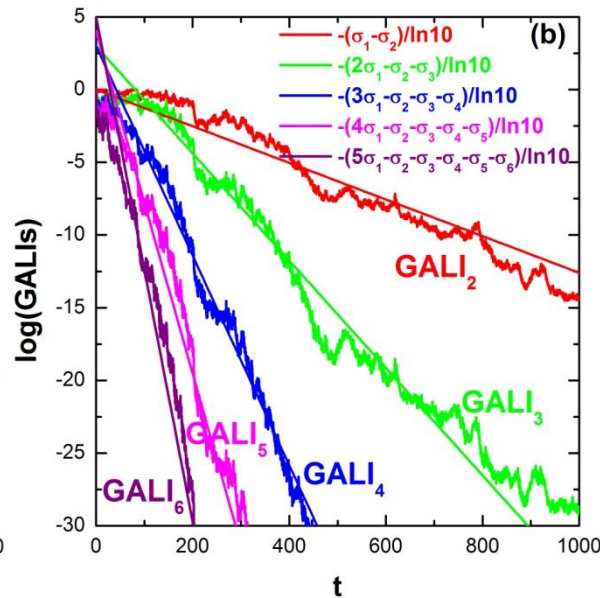
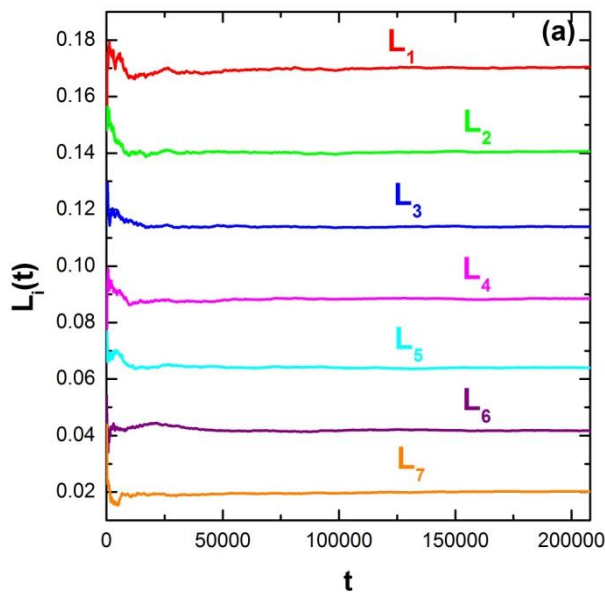


Behavior of $GALI_k$ for chaotic motion

N particles Fermi-Pasta-Ulam (FPU) system:

$$H = \frac{1}{2} \sum_{i=1}^N p_i^2 + \sum_{i=0}^N \left[\frac{1}{2} (q_{i+1} - q_i)^2 + \frac{\beta}{4} (q_{i+1} - q_i)^4 \right]$$

with fixed boundary conditions, $N=8$ and $\beta=1.5$.



Behavior of $GALI_k$ for regular motion

If the motion occurs on an s -dimensional torus with $s \leq N$ then the behavior of $GALI_k$ is given by (Ch.S., Bountis, Antonopoulos, 2008, Eur. Phys. J. Sp. Top.):

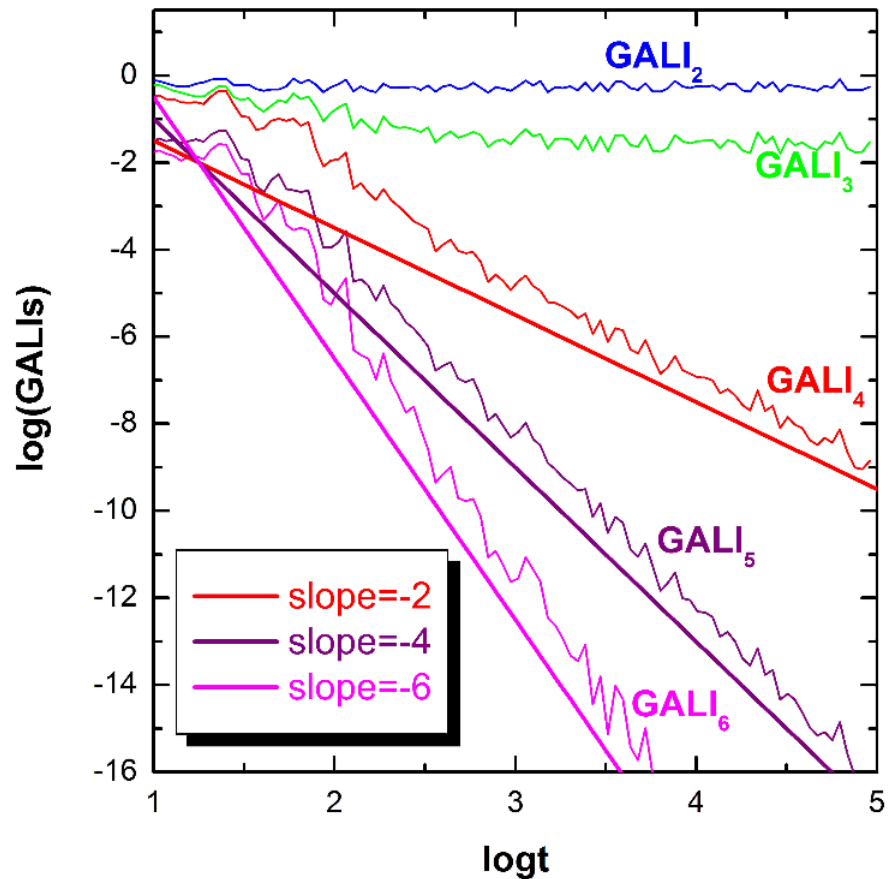
$$GALI_k(t) \propto \begin{cases} \text{constant} & \text{if } 2 \leq k \leq s \\ \frac{1}{t^{k-s}} & \text{if } s < k \leq 2N - s \\ \frac{1}{t^{2(k-N)}} & \text{if } 2N - s < k \leq 2N \end{cases}$$

while in the common case with $s=N$ we have :

$$GALI_k(t) \propto \begin{cases} \text{constant} & \text{if } 2 \leq k \leq N \\ \frac{1}{t^{2(k-N)}} & \text{if } N < k \leq 2N \end{cases}$$

Behavior of $GALI_k$ for regular motion

3D Hamiltonian



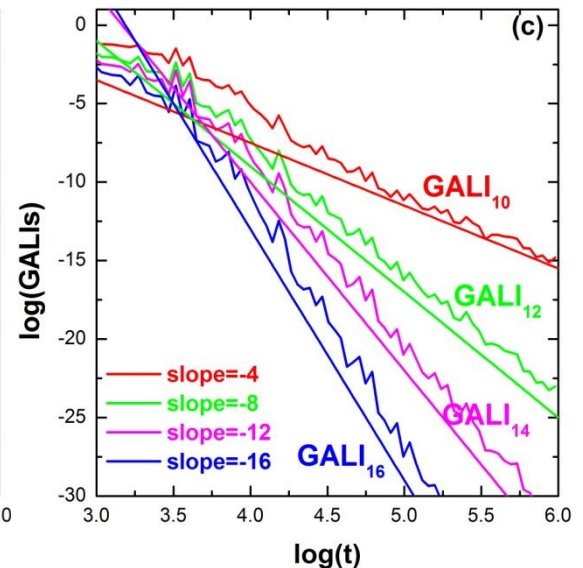
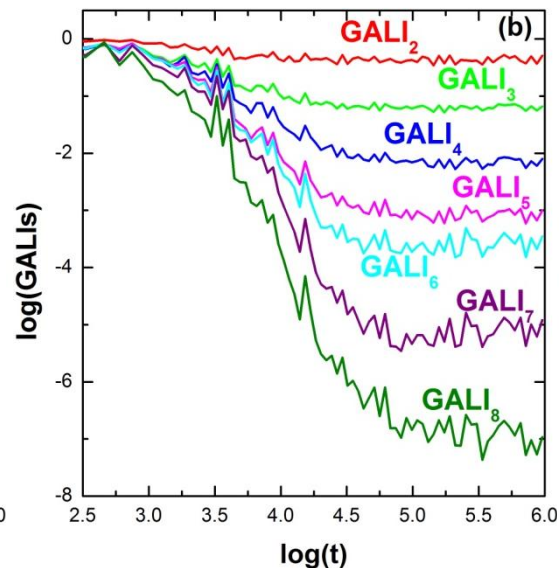
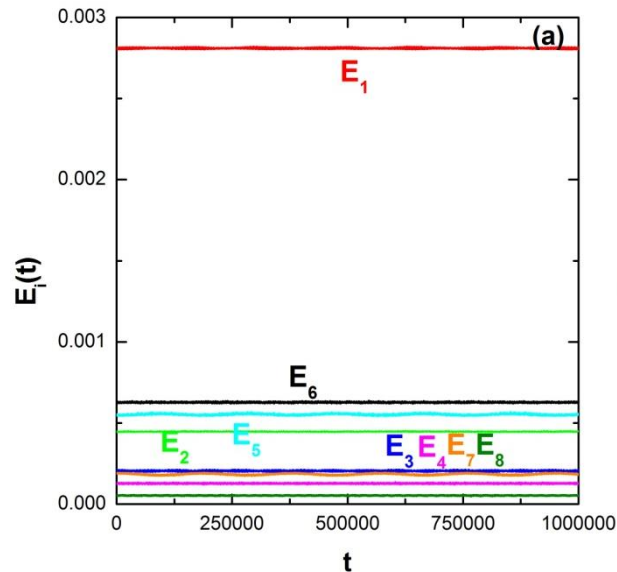
Behavior of $GALI_k$ for regular motion

N=8 FPU system: The unperturbed Hamiltonian ($\beta=0$) is written as a sum of the so-called **harmonic energies E_i** :

$$E_i = \frac{1}{2} (P_i^2 + \omega_i^2 Q_i^2), \quad i = 1, \dots, N$$

with:

$$Q_i = \sqrt{\frac{2}{N+1}} \sum_{k=1}^N q_k \sin\left(\frac{ki\pi}{N+1}\right), \quad P_i = \sqrt{\frac{2}{N+1}} \sum_{k=1}^N p_k \sin\left(\frac{ki\pi}{N+1}\right), \quad \omega_i = 2 \sin\left(\frac{i\pi}{2(N+1)}\right)$$



Global dynamics

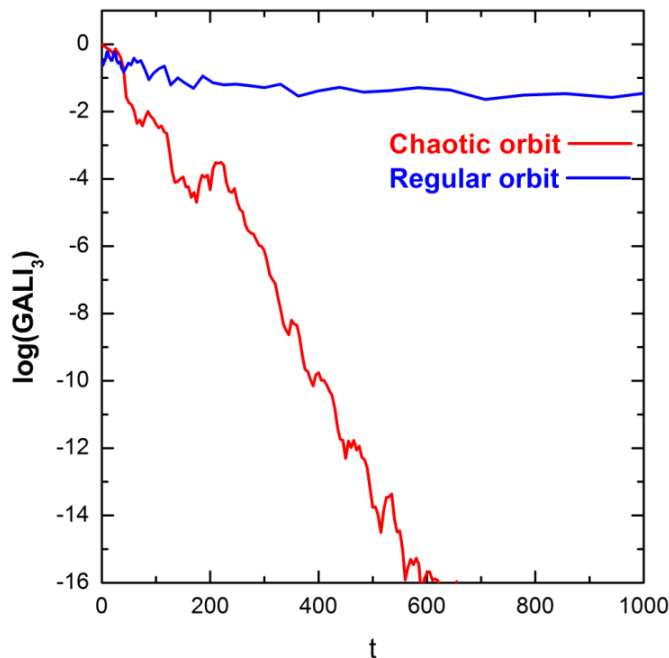
- $GALI_2$ (practically equivalent to the use of SALI)

- $GALI_N$

**Chaotic motion: $GALI_N \rightarrow 0$
(exponential decay)**

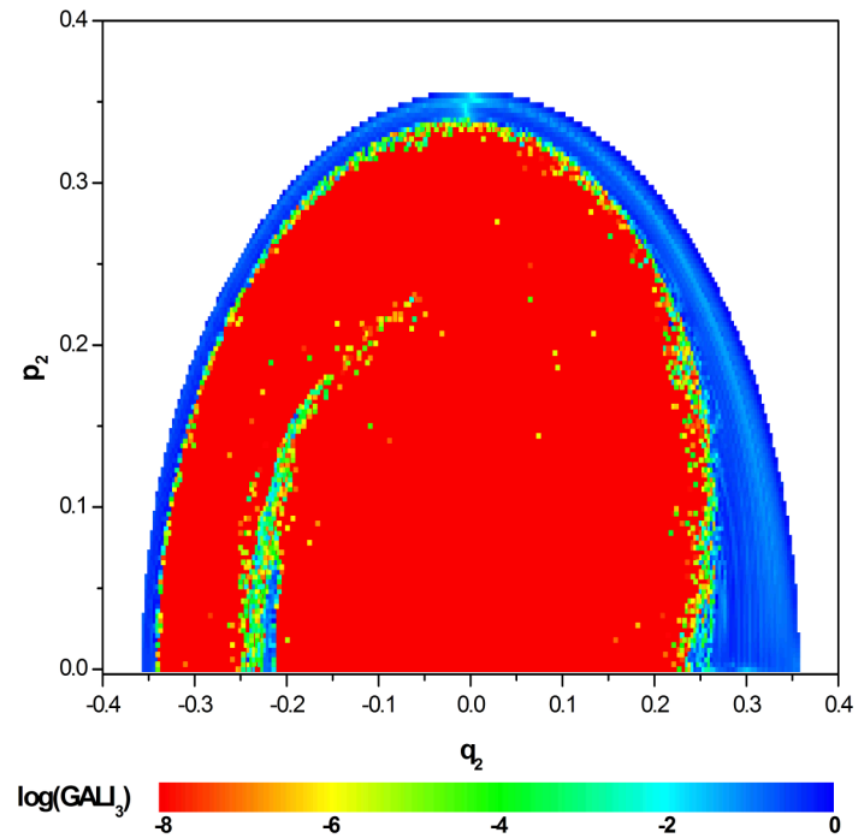
Regular motion:

$GALI_N \rightarrow \text{constant} \neq 0$



3D Hamiltonian

Subspace $q_3=p_3=0$, $p_2 \geq 0$ for $t=1000$.



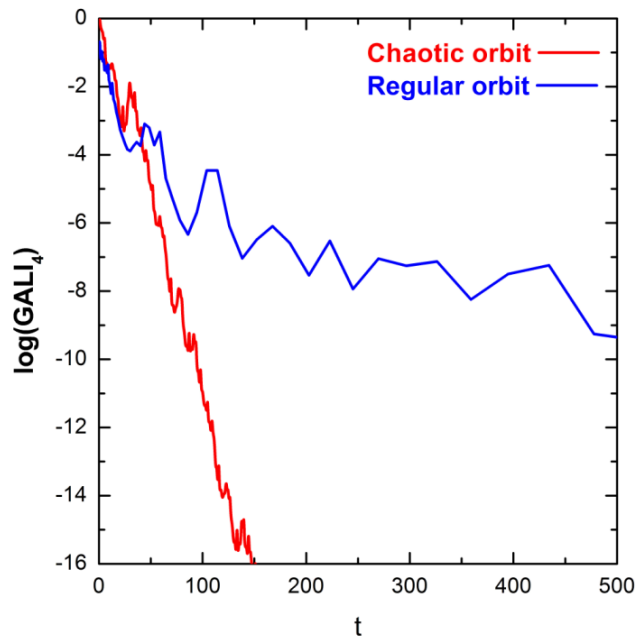
Global dynamics

$GALI_k$ with $k > N$

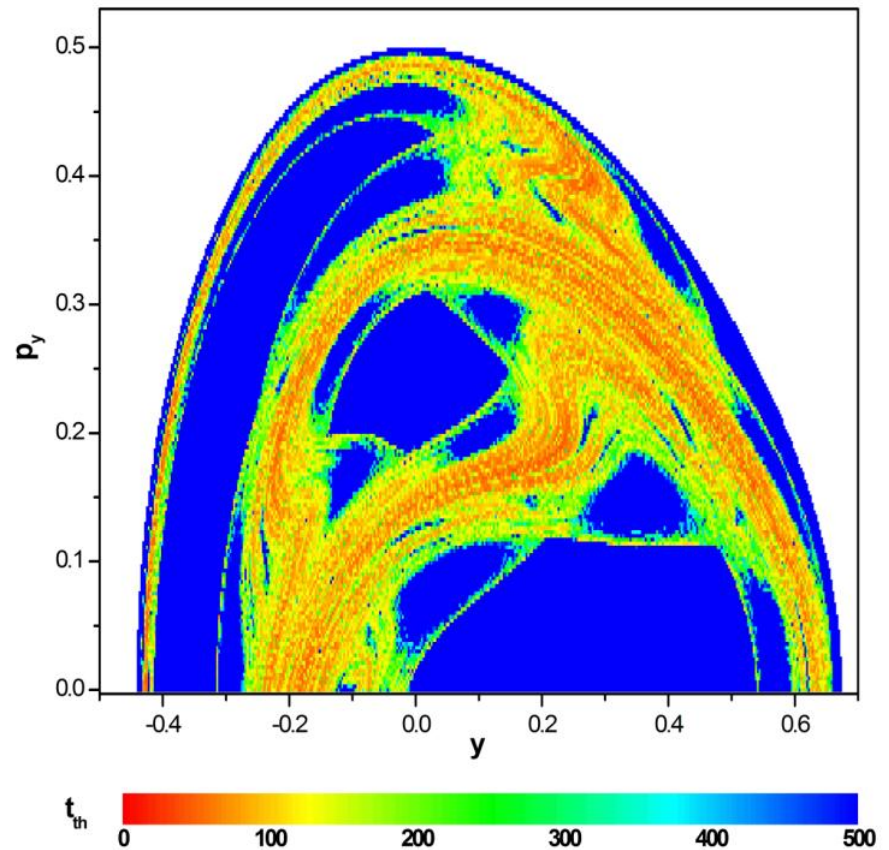
The index tends to zero both for regular and chaotic orbits but with completely different time rates:

Chaotic motion: exponential decay

Regular motion: power law



2D Hamiltonian (Hénon-Heiles) Time needed for $GALI_4 < 10^{-12}$



Behavior of $GALI_k$

Chaotic motion:

$GALI_k \rightarrow 0$ exponential decay

$$GALI_k(t) \propto e^{-[(\sigma_1 - \sigma_2) + (\sigma_1 - \sigma_3) + \dots + (\sigma_1 - \sigma_k)]t}$$

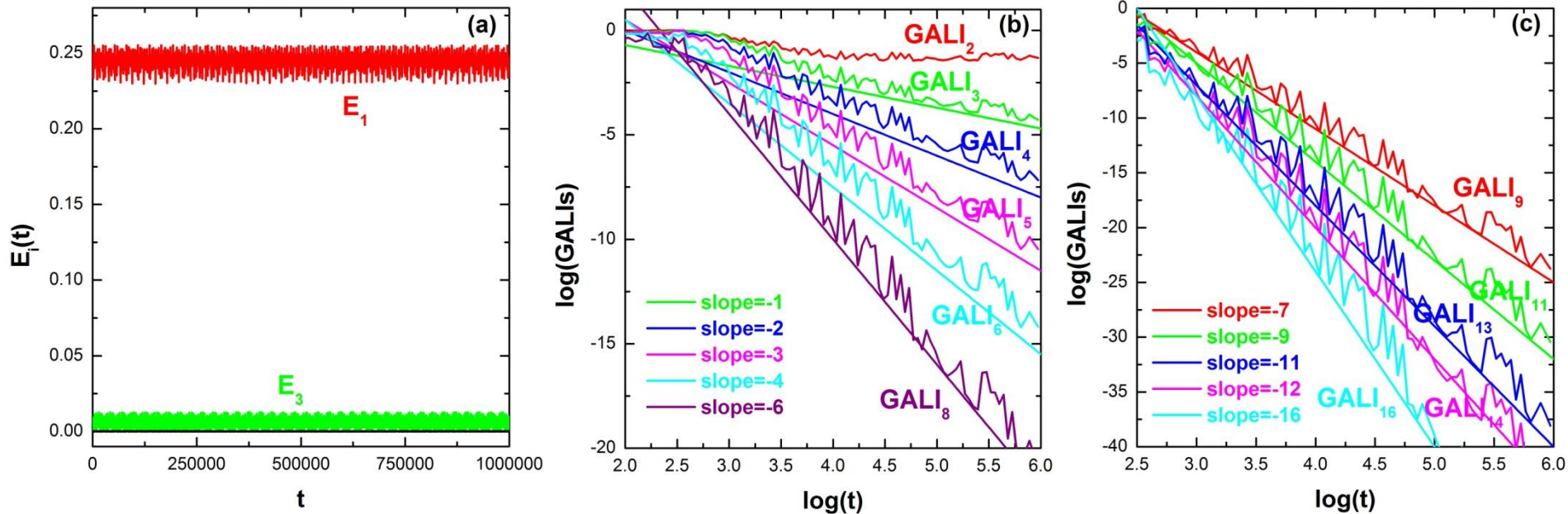
Regular motion:

$GALI_k \rightarrow \text{constant} \neq 0$ or $GALI_k \rightarrow 0$ power law decay

$$GALI_k(t) \propto \begin{cases} \text{constant} & \text{if } 2 \leq k \leq s \\ \frac{1}{t^{k-s}} & \text{if } s < k \leq 2N - s \\ \frac{1}{t^{2(k-N)}} & \text{if } 2N - s < k \leq 2N \end{cases}$$

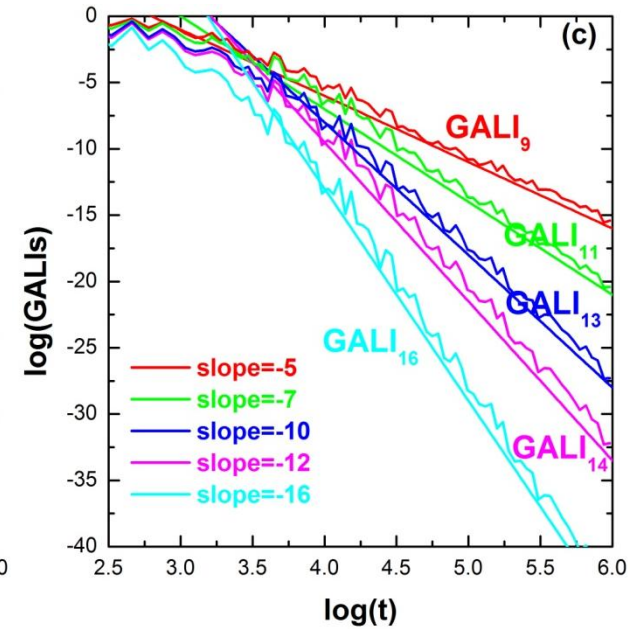
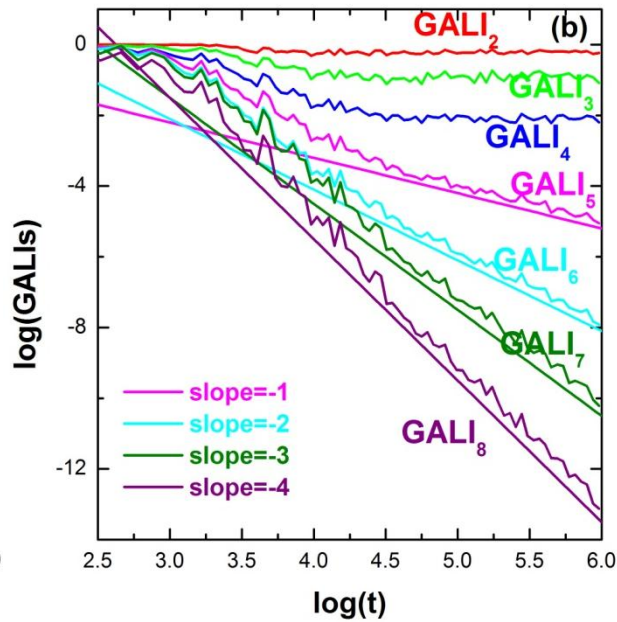
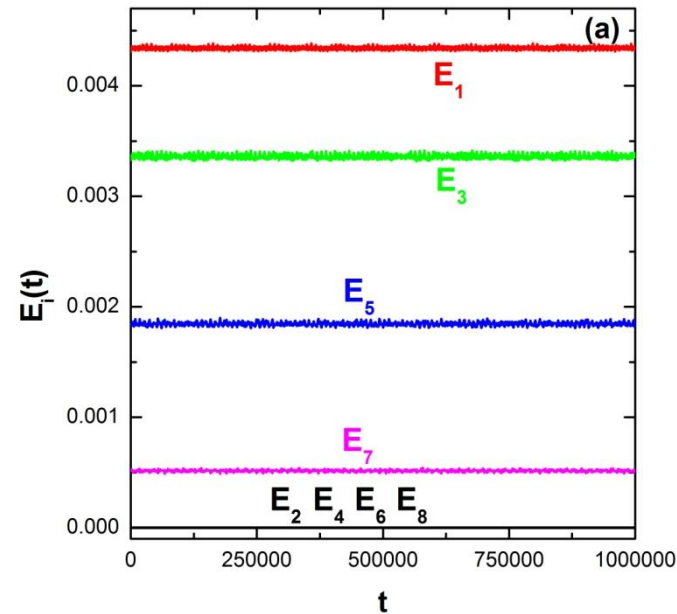
Regular motion on low-dimensional tori

A regular orbit lying on a **2-dimensional torus** for the $N=8$ FPU system.



Regular motion on low-dimensional tori

A regular orbit lying on a **4-dimensional torus** for the $N=8$ FPU system.



Low-dimensional tori - 6D map

$$\mathbf{x}'_1 = \mathbf{x}_1 + \mathbf{x}'_2$$

$$\mathbf{x}'_2 = \mathbf{x}_2 + \frac{K_1}{2\pi} \sin(2\pi\mathbf{x}_1) - \frac{B}{2\pi} \{ \sin[2\pi(\mathbf{x}_5 - \mathbf{x}_1)] + \sin[2\pi(\mathbf{x}_3 - \mathbf{x}_1)] \}$$

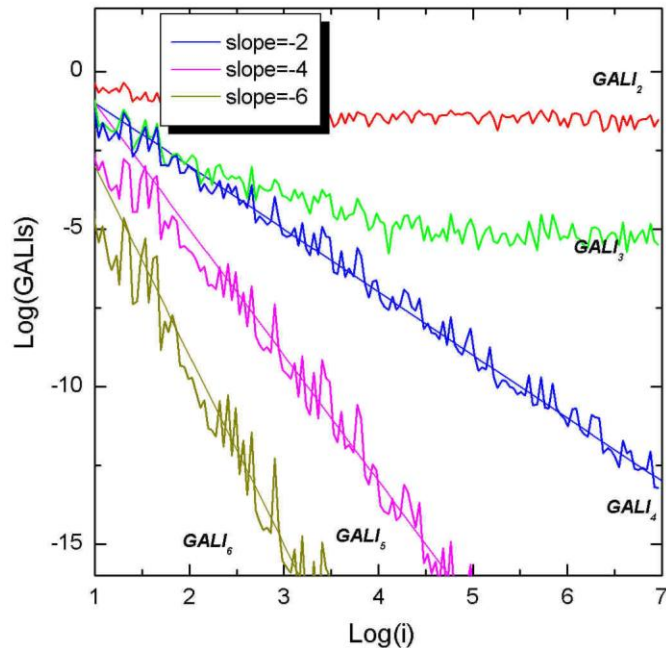
$$\mathbf{x}'_3 = \mathbf{x}_3 + \mathbf{x}'_4$$

$$\mathbf{x}'_4 = \mathbf{x}_4 + \frac{K_2}{2\pi} \sin(2\pi\mathbf{x}_3) - \frac{B}{2\pi} \{ \sin[2\pi(\mathbf{x}_1 - \mathbf{x}_3)] + \sin[2\pi(\mathbf{x}_5 - \mathbf{x}_3)] \} \pmod{1}$$

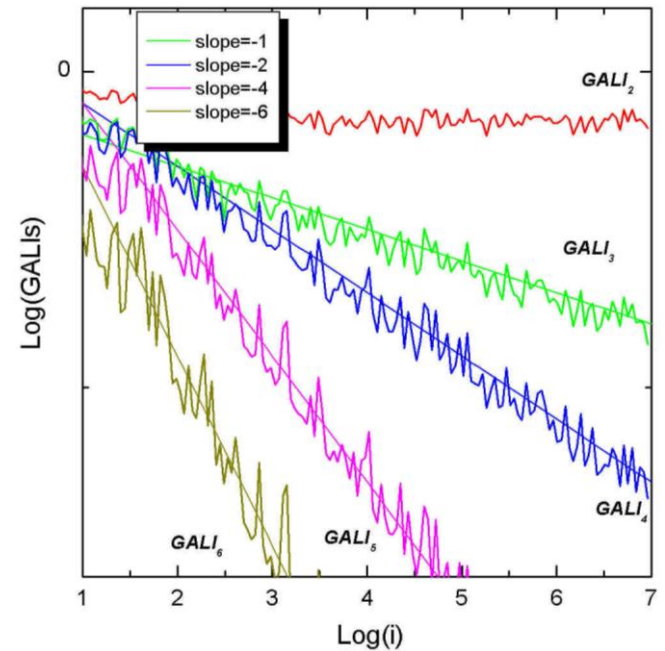
$$\mathbf{x}'_5 = \mathbf{x}_5 + \mathbf{x}'_6$$

$$\mathbf{x}'_6 = \mathbf{x}_6 + \frac{K_3}{2\pi} \sin(2\pi\mathbf{x}_5) - \frac{B}{2\pi} \{ \sin[2\pi(\mathbf{x}_3 - \mathbf{x}_5)] + \sin[2\pi(\mathbf{x}_1 - \mathbf{x}_5)] \}$$

3D torus

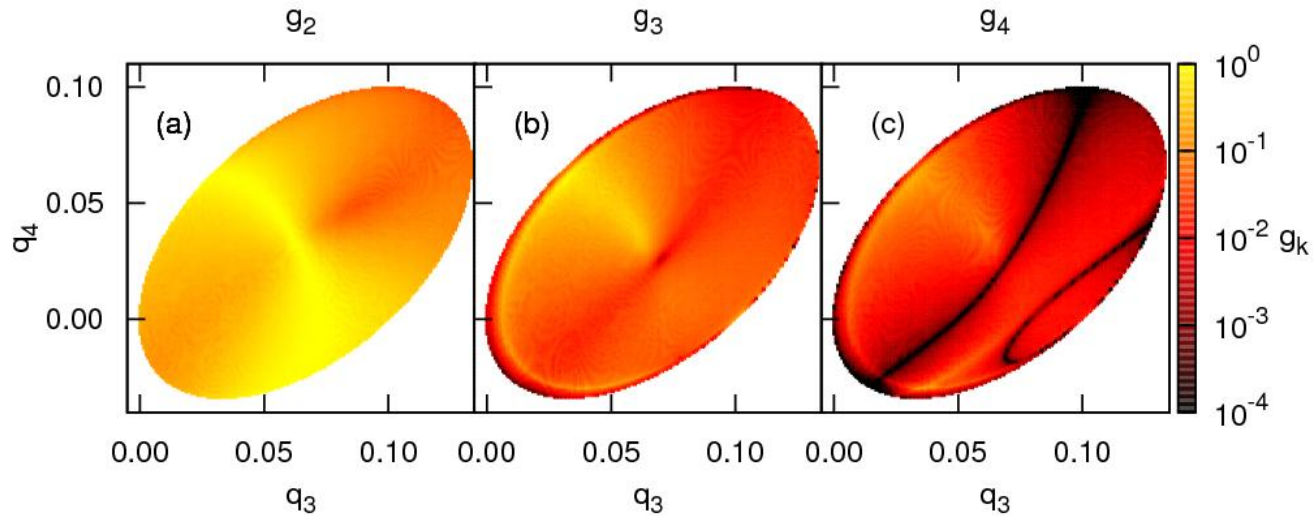


2D torus



Locating low-dimensional tori

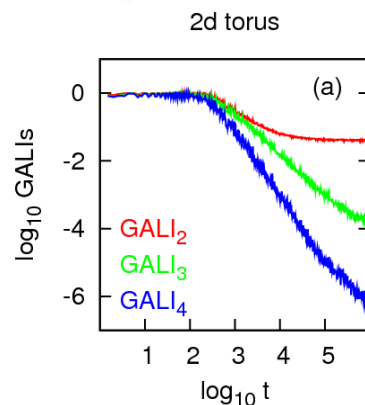
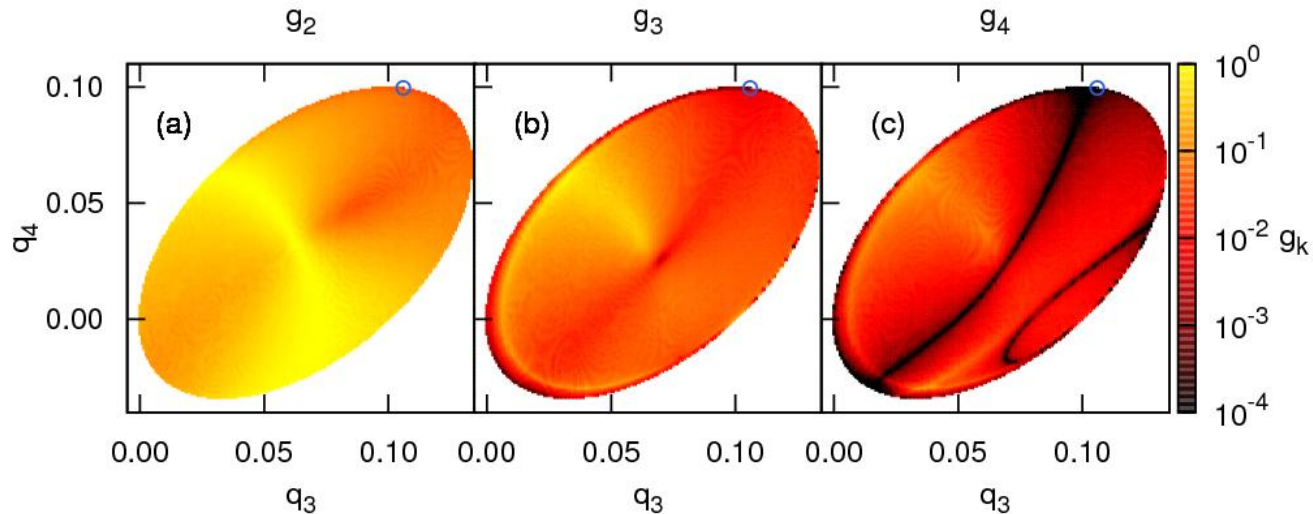
Orbits with $q_1=q_2=0.1$, $p_1=p_2=p_3=0$, $H=0.010075$ for the $N=4$ FPU system (Gerlach, Eggl, Ch.S., 2012, Int. J. Bifur. Chaos).



$$g_k = \frac{\text{GALI}_k}{\max(\text{GALI}_k)}$$

Locating low-dimensional tori

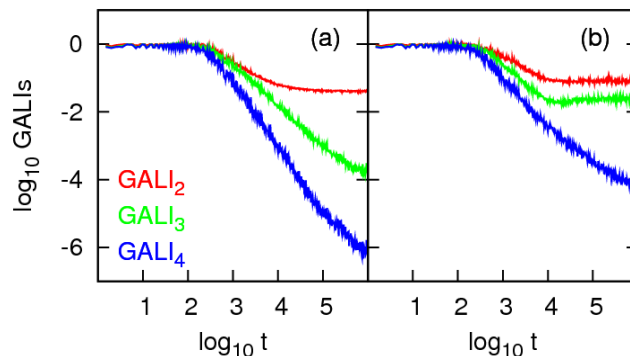
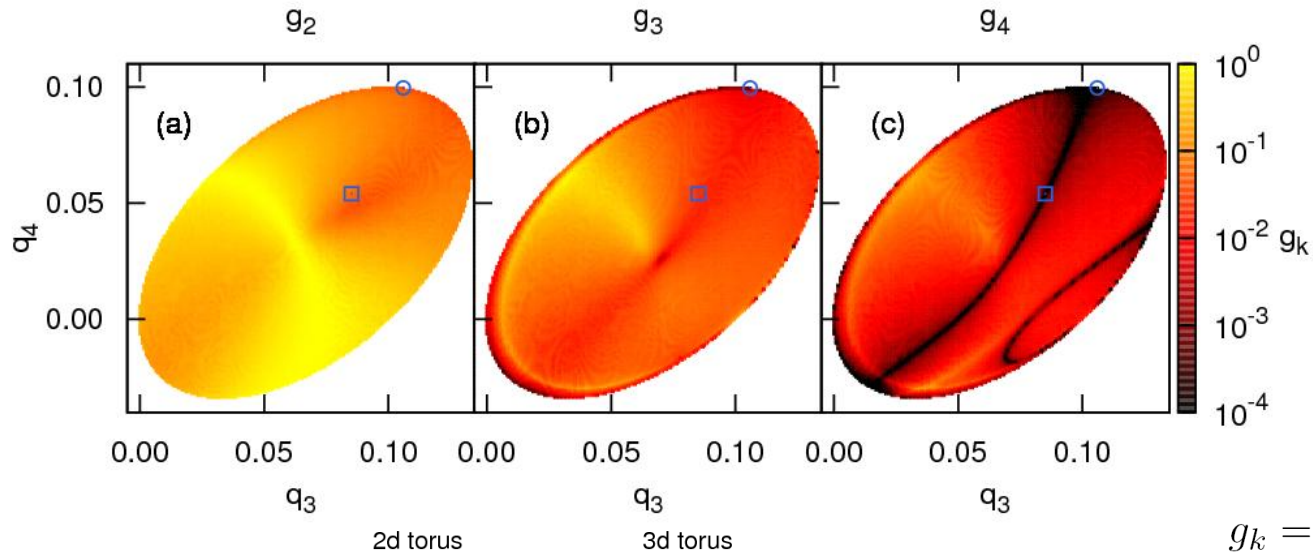
Orbits with $q_1=q_2=0.1$, $p_1=p_2=p_3=0$, $H=0.010075$ for the $N=4$ FPU system (Gerlach, Eggl, Ch.S., 2012, Int. J. Bifur. Chaos).



$$g_k = \frac{\text{GALI}_k}{\max(\text{GALI}_k)}$$

Locating low-dimensional tori

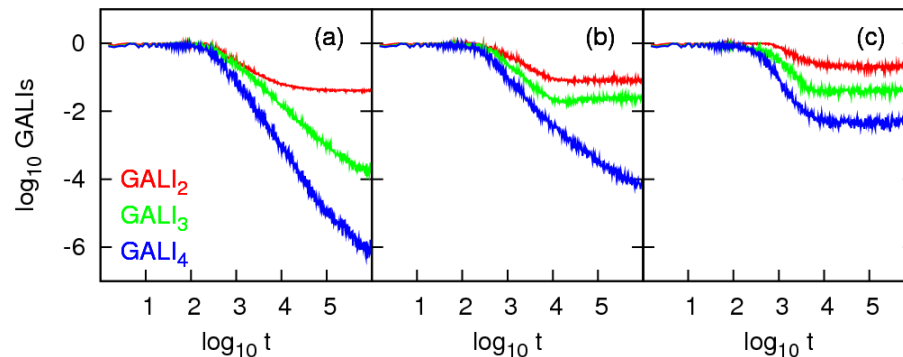
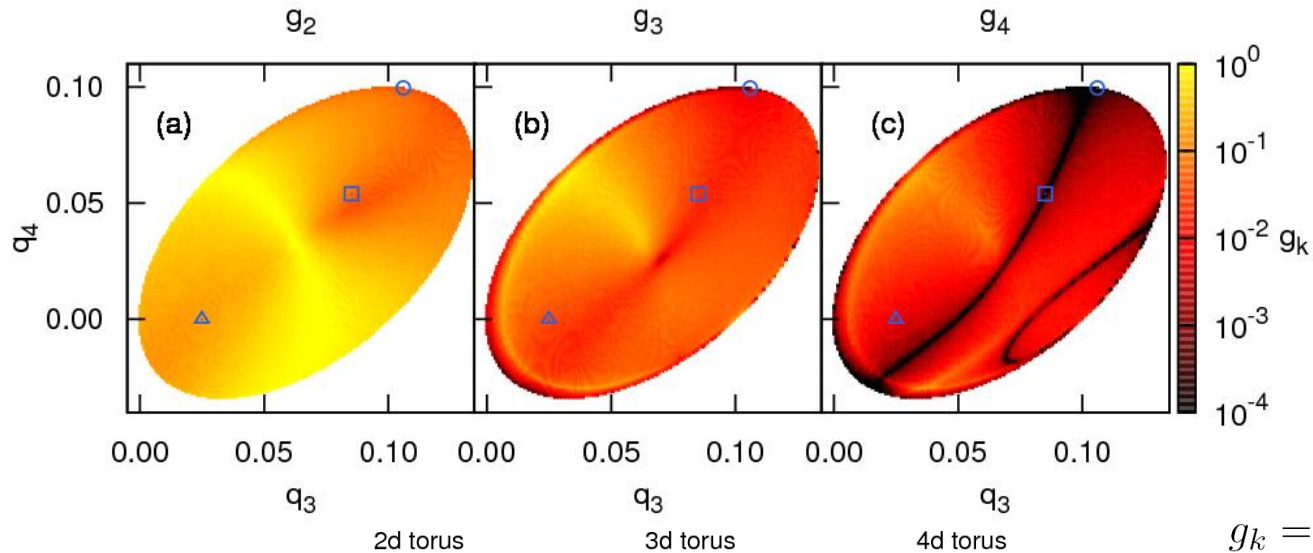
Orbits with $q_1=q_2=0.1$, $p_1=p_2=p_3=0$, $H=0.010075$ for the $N=4$ FPU system (Gerlach, Eggl, Ch.S., 2012, Int. J. Bifur. Chaos).



$$g_k = \frac{\text{GALI}_k}{\max(\text{GALI}_k)}$$

Locating low-dimensional tori

Orbits with $q_1=q_2=0.1$, $p_1=p_2=p_3=0$, $H=0.010075$ for the $N=4$ FPU system (Gerlach, Eggl, Ch.S., 2012, Int. J. Bifur. Chaos).



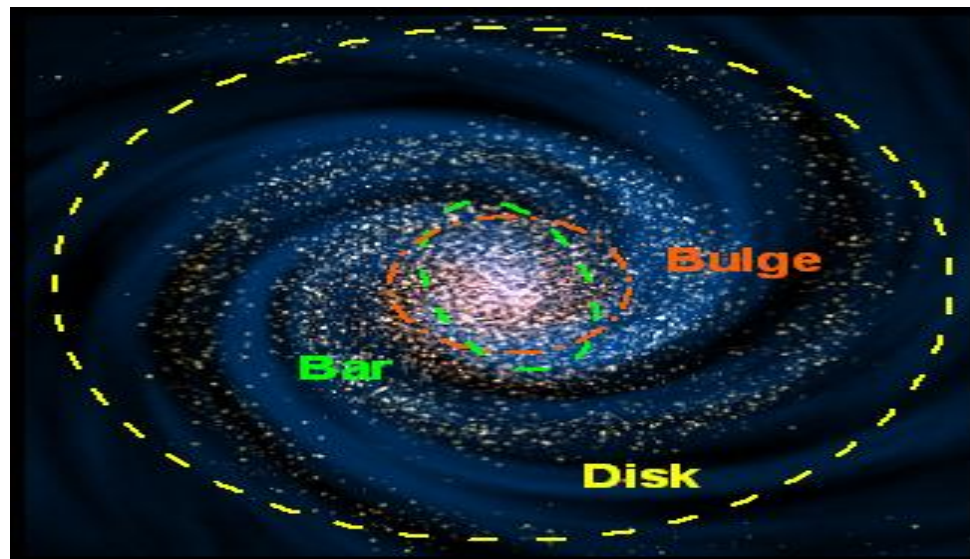
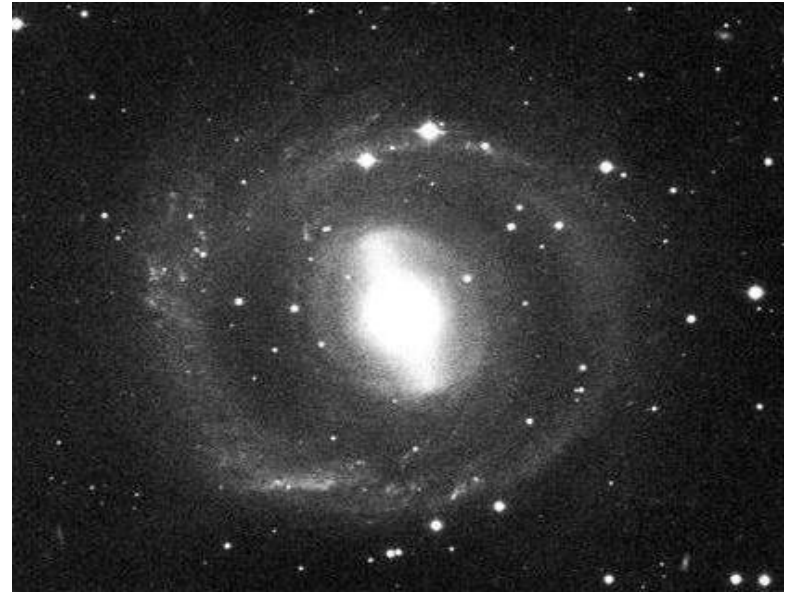
$$g_k = \frac{\text{GALI}_k}{\max(\text{GALI}_k)}$$

Barred galaxies

NGC 1433



NGC 2217



Barred galaxy model

The 3D bar rotates around its short z -axis (x : long axis and y : intermediate). The Hamiltonian that describes the motion for this model is:

$$H = \frac{1}{2}(p_x^2 + p_y^2 + p_z^2) + V(x, y, z) - \Omega_b(xp_y - yp_x) \equiv \text{Energy}$$

This model consists of the superposition of potentials describing an **axisymmetric** part and a **bar** component of the galaxy (**Manos, Bountis, Ch.S., 2013, J. Phys. A**).

a) Axisymmetric component:

i) Plummer sphere:

$$V_{\text{sphere}}(x, y, z) = -\frac{GM_S}{\sqrt{x^2 + y^2 + z^2 + \epsilon_s^2}}$$

ii) Miyamoto–Nagai disc:

$$V_{\text{disc}}(x, y, z) = -\frac{GM_D}{\sqrt{x^2 + y^2 + (A + \sqrt{B^2 + z^2})^2}}$$

b) Bar component: $V_{\text{bar}}(x, y, z) = -\pi Gabc \frac{\rho_c}{n+1} \int_{\lambda}^{\infty} \frac{du}{\Delta(u)} (1 - m^2(u))^{n+1}$,

(Ferrers bar)

$$\rho_c = \frac{105}{32\pi} \frac{GM_B}{abc}$$

where $m^2(u) = \frac{x^2}{a^2 + u} + \frac{y^2}{b^2 + u} + \frac{z^2}{c^2 + u}$, $\Delta^2(u) = (a^2 + u)(b^2 + u)(c^2 + u)$,

n : positive integer ($n = 2$ for our model), λ : the unique positive solution of $m^2(\lambda) = 1$

Its density is:

$$\rho = \begin{cases} \rho_c (1 - m^2)^n, & \text{for } m \leq 1 \\ 0, & \text{for } m > 1 \end{cases}, \text{ where } m^2 = \frac{x^2}{a^2} + \frac{y^2}{b^2} + \frac{z^2}{c^2}, \text{ } a > b > c \text{ and } n = 2.$$

Time-dependent barred galaxy model

The 3D bar rotates around its short z -axis (x : long axis and y : intermediate). The Hamiltonian that describes the motion for this model is:

$$H = \frac{1}{2}(p_x^2 + p_y^2 + p_z^2) + V(x, y, z, t) - \Omega_b(xp_y - yp_x) \equiv \text{Energy}$$

This model consists of the superposition of potentials describing an **axisymmetric** part and a **bar** component of the galaxy (**Manos, Bountis, Ch.S., 2013, J. Phys. A**).

a) Axisymmetric component:

$$M_S + M_B(t) + M_D(t) = 1, \text{ with } M_B(t) = M_B(0) + \alpha t$$

i) Plummer sphere:

$$V_{sphere}(x, y, z) = -\frac{GM_S}{\sqrt{x^2 + y^2 + z^2 + \epsilon_s^2}}$$

ii) Miyamoto–Nagai disc:

$$V_{disc}(x, y, z) = -\frac{GM_D(t)}{\sqrt{x^2 + y^2 + (A + \sqrt{B^2 + z^2})^2}}$$

b) Bar component: $V_{bar}(x, y, z) = -\pi Gabc \frac{\rho_c}{n+1} \int_{\lambda}^{\infty} \frac{du}{\Delta(u)} (1 - m^2(u))^{n+1}$,

(Ferrers bar)

$$\text{where } m^2(u) = \frac{x^2}{a^2 + u} + \frac{y^2}{b^2 + u} + \frac{z^2}{c^2 + u}, \Delta^2(u) = (a^2 + u)(b^2 + u)(c^2 + u),$$

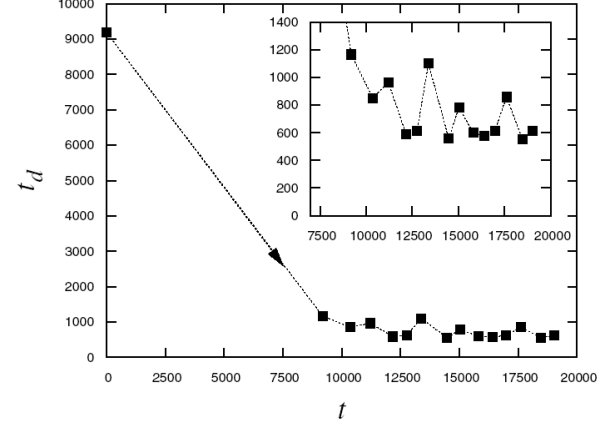
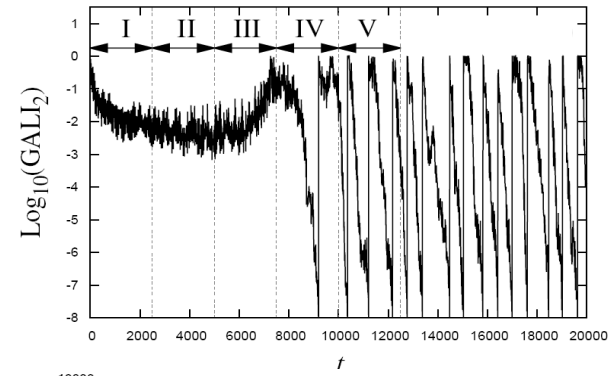
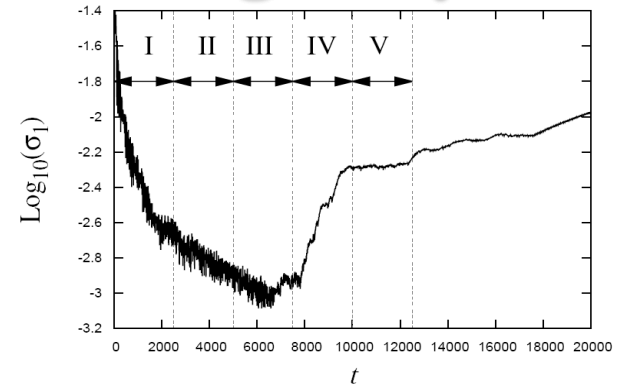
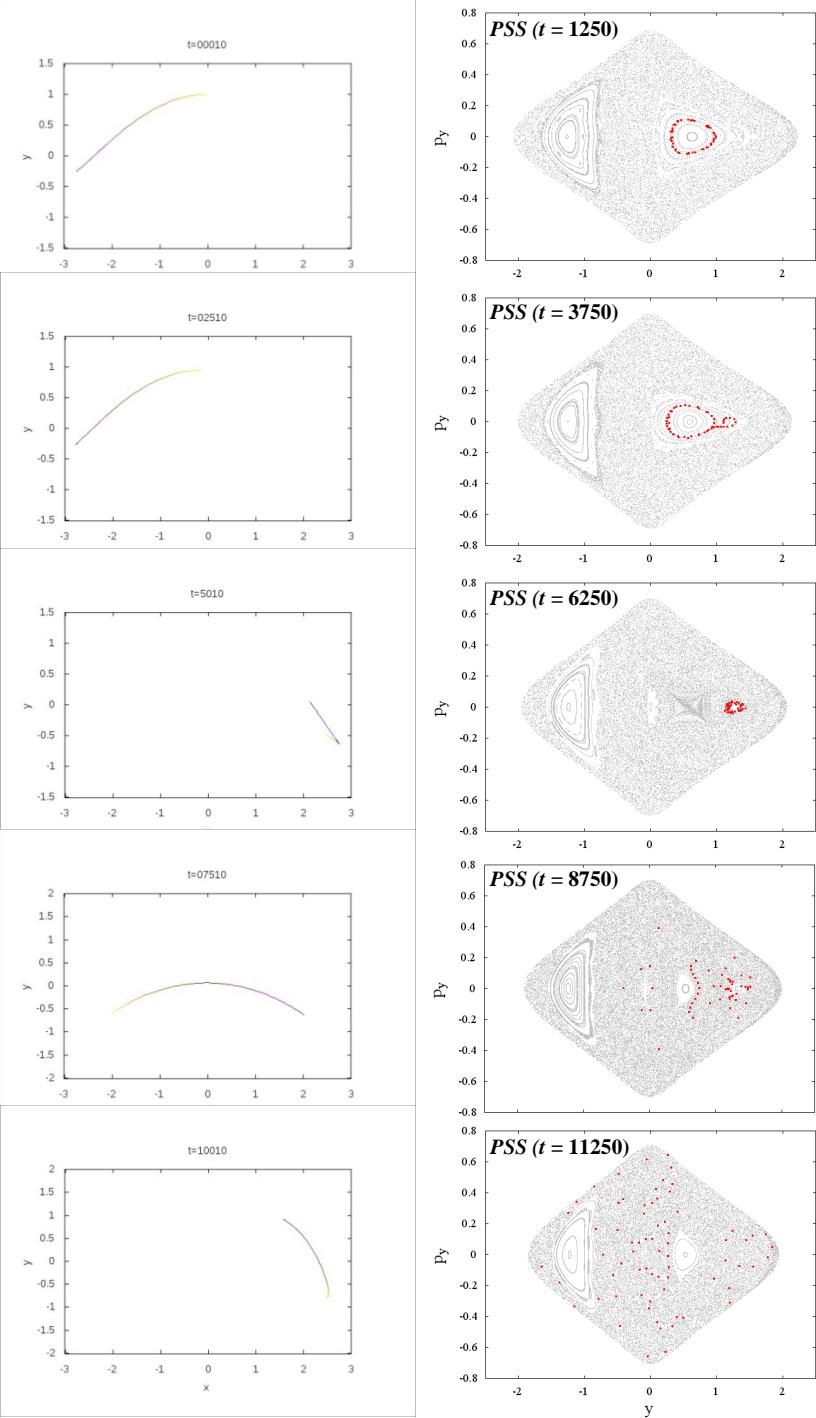
$$\rho_c = \frac{105}{32\pi} \frac{GM_B(t)}{abc}$$

n : positive integer ($n = 2$ for our model), λ : the unique positive solution of $m^2(\lambda) = 1$

Its density is:

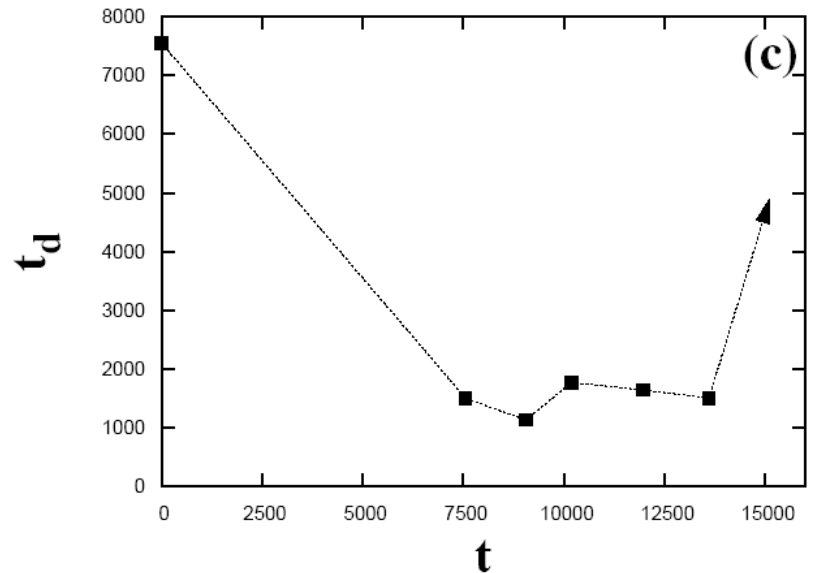
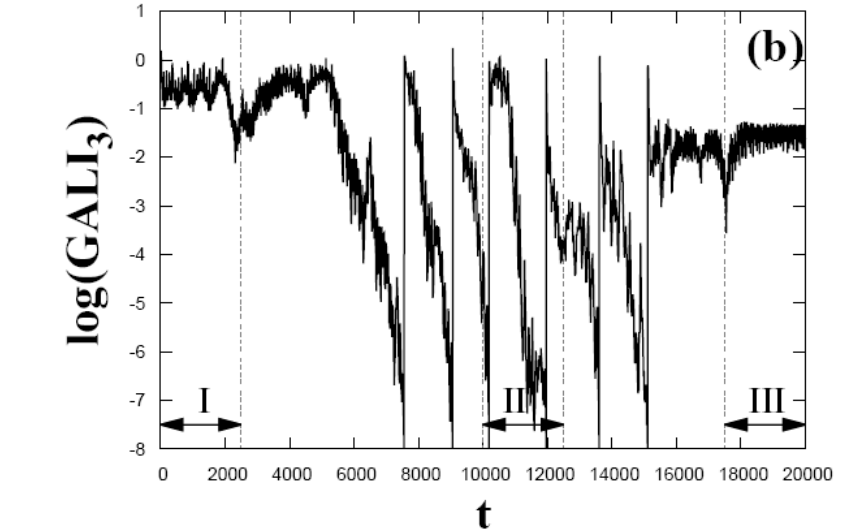
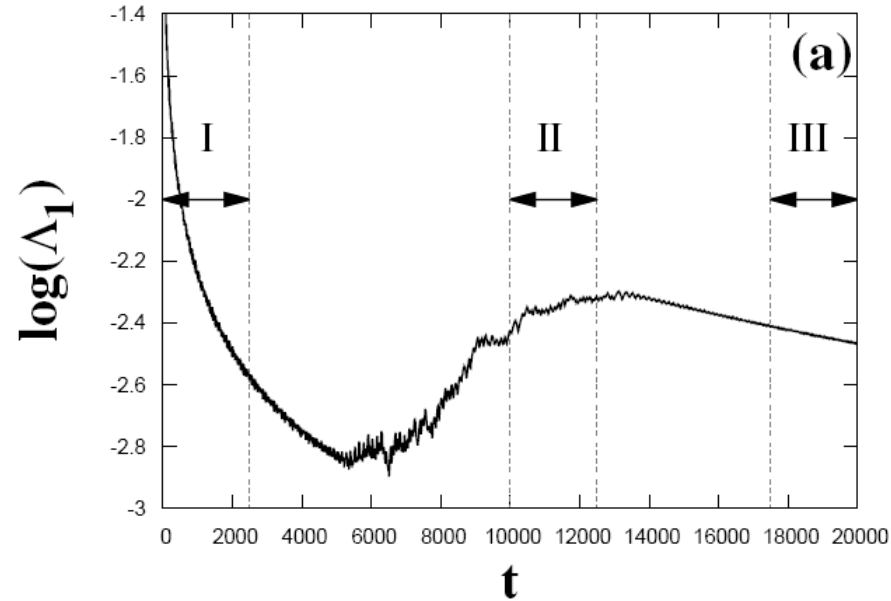
$$\rho = \begin{cases} \rho_c (1 - m^2)^n, & \text{for } m \leq 1 \\ 0, & \text{for } m > 1 \end{cases}, \text{ where } m^2 = \frac{x^2}{a^2} + \frac{y^2}{b^2} + \frac{z^2}{c^2}, a > b > c \text{ and } n = 2.$$

Time-dependent 2D barred galaxy model



Time-dependent 3D barred galaxy model

Interplay between chaotic and regular motion



Numerical Integration of Equations of Motion and Variational Equations

Efficient integration of variational equations

Consider an **N degree of freedom** autonomous Hamiltonian system having a Hamiltonian function of the form:

$$H(\vec{q}, \vec{p}) = \frac{1}{2} \sum_{i=1}^N p_i^2 + V(\vec{q})$$

with $\vec{q} = (q_1(t), q_2(t), \dots, q_N(t))$ $\vec{p} = (p_1(t), p_2(t), \dots, p_N(t))$ being respectively the coordinates and momenta.

The time evolution of an orbit is governed by the **Hamilton's equations of motion**

$$\begin{aligned}\dot{\vec{q}} &= \vec{p} \\ \dot{\vec{p}} &= -\frac{\partial V}{\partial \vec{q}}\end{aligned}$$

Variational Equations

The time evolution of a **deviation vector**

$$\vec{w}(t) = (\delta q_1(t), \delta q_2(t), \dots, \delta q_N(t), \delta p_1(t), \delta p_2(t), \dots, \delta p_N(t))$$

from a given orbit is governed by the **variational equations**:

$$\begin{aligned}\dot{\delta \vec{q}} &= \delta \vec{p} \\ \dot{\delta \vec{p}} &= -\mathbf{D}^2 \mathbf{V}(\vec{q}(t)) \delta \vec{q}\end{aligned}$$

where $\mathbf{D}^2 \mathbf{V}(\vec{q}(t))_{jk} = \left. \frac{\partial^2 V(\vec{q})}{\partial q_j \partial q_k} \right|_{\vec{q}(t)}$, $j, k = 1, 2, \dots, N$.

The variational equations are the equations of motion of the time dependent **tangent dynamics Hamiltonian (TDH) function**

$$H_V(\delta \vec{q}, \delta \vec{p}; t) = \frac{1}{2} \sum_{j=1}^N \delta p_j^2 + \frac{1}{2} \sum_{j,k} \mathbf{D}^2 \mathbf{V}(\vec{q}(t))_{jk} \delta q_j \delta q_k$$

Autonomous Hamiltonian systems

As an example, we consider the Hénon-Heiles system:

$$H_2 = \frac{1}{2}(p_x^2 + p_y^2) + \frac{1}{2}(x^2 + y^2) + x^2y - \frac{1}{3}y^3$$

Hamilton's equations of motion:

$$\begin{cases} \dot{x} &= p_x \\ \dot{y} &= p_y \\ \dot{p}_x &= -x - 2xy \\ \dot{p}_y &= y^2 - x^2 - y \end{cases}$$

Variational equations:

$$\begin{cases} \delta\dot{x} &= \delta p_x \\ \delta\dot{y} &= \delta p_y \\ \delta\dot{p}_x &= -(1 + 2y)\delta x - 2x\delta y \\ \delta\dot{p}_y &= -2x\delta x + (-1 + 2y)\delta y \end{cases}$$

Integration of the variational equations

We use two general-purpose **numerical integration algorithms for the integration of the whole set of equations:**

$$\left\{ \begin{array}{l} \dot{x} = p_x \\ \dot{y} = p_y \\ \dot{p}_x = -x - 2xy \\ \dot{p}_y = y^2 - x^2 - y \\ \delta \dot{x} = \delta p_x \\ \delta \dot{y} = \delta p_y \\ \delta \dot{p}_x = -(1 + 2y)\delta x - 2x\delta y \\ \delta \dot{p}_y = -2x\delta x + (-1 + 2y)\delta y \end{array} \right.$$

a) the **DOP853 integrator** (Hairer et al. 1993, <http://www.unige.ch/~hairer/software.html>), which is an explicit non-symplectic Runge-Kutta integration scheme of order 8,

b) the **TIDES integrator** (Barrio 2005, <http://gme.unizar.es/software/tides>), which is based on a Taylor series approximation

$$\mathbf{y}(t_i + \tau) \simeq \mathbf{y}(t_i) + \tau \frac{d\mathbf{y}(t_i)}{dt} + \frac{\tau^2}{2!} \frac{d^2\mathbf{y}(t_i)}{dt^2} + \dots + \frac{\tau^n}{n!} \frac{d^n\mathbf{y}(t_i)}{dt^n}$$

for the solution of system

$$\frac{d\mathbf{y}(t)}{dt} = \mathbf{f}(\mathbf{y}(t))$$

Symplectic Integration schemes

Formally the solution of the Hamilton's equations of motion can be written as:

$$\frac{d\vec{X}}{dt} = \{H, \vec{X}\} = L_H \vec{X} \Rightarrow \vec{X}(t) = \sum_{n \geq 0} \frac{t^n}{n!} L_H^n \vec{X} = e^{tL_H} \vec{X}$$

where \vec{X} is the full coordinate vector and L_H the Poisson operator:

$$L_H f = \sum_{j=1}^N \left\{ \frac{\partial H}{\partial p_j} \frac{\partial f}{\partial q_j} - \frac{\partial H}{\partial q_j} \frac{\partial f}{\partial p_j} \right\}$$

If the Hamiltonian H can be **split into two integrable parts as $H=A+B$** , a symplectic scheme for integrating the equations of motion **from time t to time $t+\tau$** consists of approximating the operator $e^{\tau L_H}$ by

$$e^{\tau L_H} = e^{\tau(L_A + L_B)} \approx \prod_{i=1}^j e^{c_i \tau L_A} e^{d_i \tau L_B}$$

for appropriate values of constants c_i, d_i .

So the dynamics over an integration time step τ is described by a series of successive acts of Hamiltonians A and B .

Symplectic Integrator SABA₂C

We use a **symplectic integration scheme** developed for Hamiltonians of the form $H=A+\varepsilon B$ where A, B are both integrable and ε a parameter. The operator $e^{\tau L_H}$ can be approximated by the symplectic integrator (Laskar & Robutel, 2001, Cel. Mech. Dyn. Astr.):

$$\mathbf{SABA}_2 = e^{c_1 \tau L_A} e^{d_1 \tau L_{\varepsilon B}} e^{c_2 \tau L_A} e^{d_1 \tau L_{\varepsilon B}} e^{c_1 \tau L_A}$$

with $c_1 = \frac{(3-\sqrt{3})}{6}$, $c_2 = \frac{\sqrt{3}}{3}$, $d_1 = \frac{1}{2}$.

The integrator has only **positive steps** and its **error is of order $O(\tau^4 \varepsilon + \tau^2 \varepsilon^2)$** .

In the case where A is quadratic in the momenta and B depends only on the positions the method can be improved by introducing a **corrector**

$C = \{\{A, B\}, B\}$, having a small negative step: $e^{-\tau^3 \varepsilon^2 \frac{c}{2} L_{\{\{A, B\}, B\}}}$

with $c = \frac{(2-\sqrt{3})}{24}$.

Thus the full integrator scheme becomes: $\mathbf{SABAC}_2 = C (\mathbf{SABA}_2) C$ and its **error is of order $O(\tau^4 \varepsilon + \tau^4 \varepsilon^2)$** .

Tangent Map (TM) Method

Use symplectic integration schemes for the whole set of equations (Ch.S., Gerlach, 2010, PRE)

We apply the **SABAC₂** integrator scheme to the Hénon-Heiles system (with $\varepsilon=1$) by using **the splitting**:

$$A = \frac{1}{2}(p_x^2 + p_y^2), \quad B = \frac{1}{2}(x^2 + y^2) + x^2y - \frac{1}{3}y^3,$$

with a **corrector term** which corresponds to the Hamiltonian function:

$$C = \{\{A, B\}, B\} = (x + 2xy)^2 + (x^2 - y^2 + y)^2$$

We approximate the dynamics by **the act of Hamiltonians A, B and C**, which correspond to the symplectic maps:

$$e^{\tau L_A} : \begin{cases} x' = x + p_x \tau \\ y' = y + p_y \tau \\ p'_x = p_x \\ p'_y = p_y \end{cases}, \quad e^{\tau L_C} : \begin{cases} x' = x \\ y' = y \\ p'_x = p_x - 2x(1 + 2x^2 + 6y + 2y^2)\tau \\ p'_y = p_y - 2(y - 3y^2 + 2y^3 + 3x^2 + 2x^2y)\tau \end{cases}$$
$$e^{\tau L_B} : \begin{cases} x' = x \\ y' = y \\ p'_x = p_x - x(1 + 2y)\tau \\ p'_y = p_y + (y^2 - x^2 - y)\tau \end{cases},$$

Tangent Map (TM) Method

Let $\vec{u} = (x, y, p_x, p_y, \delta x, \delta y, \delta p_x, \delta p_y)$

The system of the Hamilton's equations of motion and the variational equations is **split into two integrable systems which correspond to Hamiltonians A and B.**

$$\begin{array}{l}
 \dot{x} = p_x \\
 \dot{y} = p_y \\
 \dot{p}_x = -x - 2xy \\
 \dot{p}_y = y^2 - x^2 - y \\
 \\
 \dot{\delta x} = \delta p_x \\
 \dot{\delta y} = \delta p_y \\
 \dot{\delta p}_x = -(1 + 2y)\delta x - 2x\delta y \\
 \dot{\delta p}_y = -2x\delta x + (-1 + 2y)\delta y
 \end{array}
 \xrightarrow{A(\vec{p})}
 \left. \begin{array}{l}
 \dot{x} = p_x \\
 \dot{y} = p_y \\
 \dot{p}_x = 0 \\
 \dot{p}_y = 0 \\
 \dot{\delta x} = \delta p_x \\
 \dot{\delta y} = \delta p_y \\
 \dot{\delta p}_x = 0 \\
 \dot{\delta p}_y = 0
 \end{array} \right\}
 \Rightarrow \frac{d\vec{u}}{dt} = L_{AV}\vec{u} \Rightarrow e^{\tau L_{AV}} : \left\{ \begin{array}{l}
 x' = x + p_x\tau \\
 y' = y + p_y\tau \\
 px' = p_x \\
 py' = p_y \\
 \delta x' = \delta x + \delta p_x\tau \\
 \delta y' = \delta y + \delta p_y\tau \\
 \delta p'_x = \delta p_x \\
 \delta p'_y = \delta p_y
 \end{array} \right.$$

$$\left. \begin{array}{l}
 \dot{x} = 0 \\
 \dot{y} = 0 \\
 \dot{p}_x = -x - 2xy \\
 \dot{p}_y = y^2 - x^2 - y \\
 \dot{\delta x} = 0 \\
 \dot{\delta y} = 0 \\
 \dot{\delta p}_x = -(1 + 2y)\delta x - 2x\delta y \\
 \dot{\delta p}_y = -2x\delta x + (-1 + 2y)\delta y
 \end{array} \right\}
 \xrightarrow{B(\vec{q})}
 \Rightarrow \frac{d\vec{u}}{dt} = L_{BV}\vec{u} \Rightarrow e^{\tau L_{BV}} : \left\{ \begin{array}{l}
 x' = x \\
 y' = y \\
 p'_x = p_x - x(1 + 2y)\tau \\
 p'_y = p_y + (y^2 - x^2 - y)\tau \\
 \delta x' = \delta x \\
 \delta y' = \delta y \\
 \delta p'_x = \delta p_x - [(1 + 2y)\delta x + 2x\delta y]\tau \\
 \delta p'_y = \delta p_y + [-2x\delta x + (-1 + 2y)\delta y]\tau
 \end{array} \right.$$

Tangent Map (TM) Method

So any symplectic integration scheme used for solving the Hamilton's equations of motion, which involves the action of Hamiltonians A, B and C, can be extended in order to integrate simultaneously the variational equations.

$$\begin{array}{ccc}
 e^{\tau L_A} : \begin{cases} x' = x + p_x \tau \\ y' = y + p_y \tau \\ p'_x = p_x \\ p'_y = p_y \end{cases} & \xrightarrow{\quad} & e^{\tau L_{AV}} : \begin{cases} x' = x + p_x \tau \\ y' = y + p_y \tau \\ p'_x = p_x \\ p'_y = p_y \\ \delta x' = \delta x + \delta p_x \tau \\ \delta y' = \delta y + \delta p_y \tau \\ \delta p'_x = \delta p_x \\ \delta p'_y = \delta p_y \end{cases} \\
 \\
 e^{\tau L_B} : \begin{cases} x' = x \\ y' = y \\ p'_x = p_x - x(1 + 2y)\tau \\ p'_y = p_y + (y^2 - x^2 - y)\tau \end{cases} & \xrightarrow{\quad} & e^{\tau L_{BV}} : \begin{cases} x' = x \\ y' = y \\ p'_x = p_x - x(1 + 2y)\tau \\ p'_y = p_y + (y^2 - x^2 - y)\tau \\ \delta x' = \delta x \\ \delta y' = \delta y \\ \delta p'_x = \delta p_x - [(1 + 2y)\delta x + 2x\delta y]\tau \\ \delta p'_y = \delta p_y + [-2x\delta x + (-1 + 2y)\delta y]\tau \end{cases} \\
 \\
 e^{\tau L_C} : \begin{cases} x' = x \\ y' = y \\ p'_x = p_x - 2x(1 + 2x^2 + 6y + 2y^2)\tau \\ p'_y = p_y - 2(y - 3y^2 + 2y^3 + 3x^2 + 2x^2y)\tau \end{cases} & \xrightarrow{\quad} & e^{\tau L_{CV}} : \begin{cases} x' = x \\ y' = y \\ p'_x = p_x - 2x(1 + 2x^2 + 6y + 2y^2)\tau \\ p'_y = p_y - 2(y - 3y^2 + 2y^3 + 3x^2 + 2x^2y)\tau \\ \delta x' = \delta x \\ \delta y' = \delta y \\ \delta p'_x = \delta p_x - 2[(1 + 6x^2 + 2y^2 + 6y)\delta x + \\ \quad + 2x(3 + 2y)\delta y]\tau \\ \delta p'_y = \delta p_y - 2[2x(3 + 2y)\delta x + \\ \quad + (1 + 2x^2 + 6y^2 - 6y)\delta y]\tau \end{cases}
 \end{array}$$

Application: FPU system

N particles Fermi-Pasta-Ulam (FPU) system:

$$H = \frac{1}{2} \sum_{i=1}^N p_i^2 + \sum_{i=0}^N \left[\frac{1}{2} (q_{i+1} - q_i)^2 + \frac{\beta}{4} (q_{i+1} - q_i)^4 \right]$$

with fixed boundary conditions, $\beta=1.5$ and $N=4 - 20$.

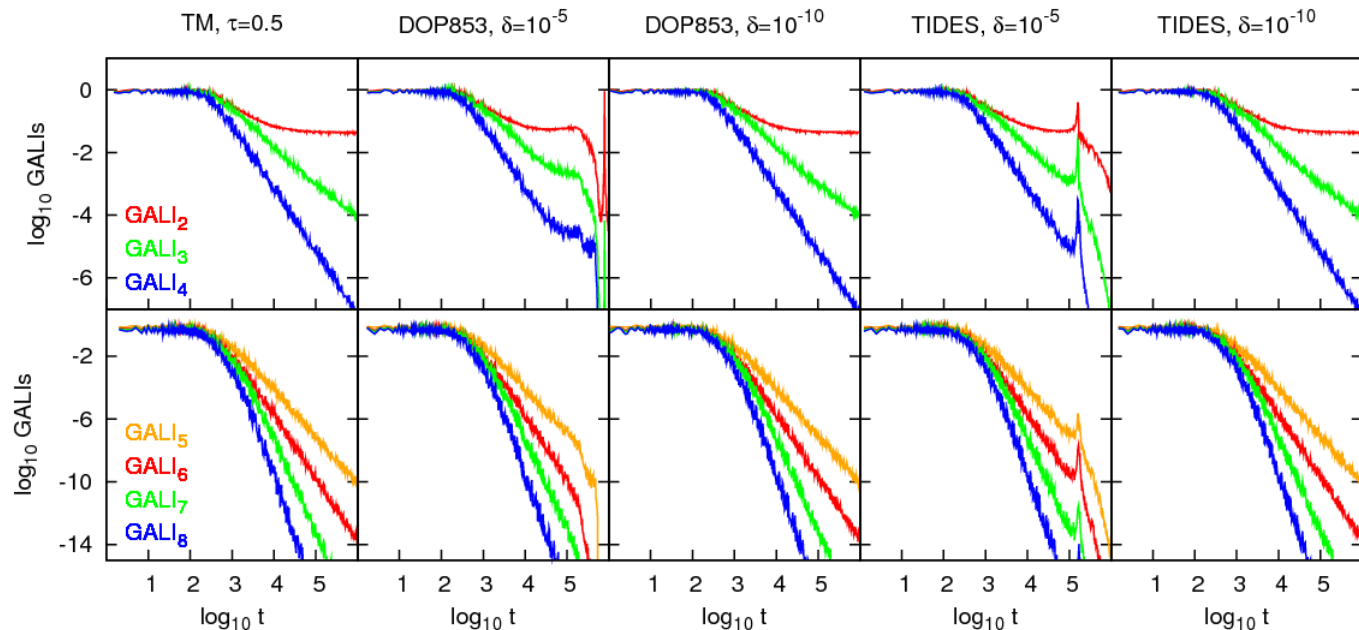
N=4. Regular motion on 2d torus. Final time $t=10^6$.

CPU times \approx

9 s

54 s

1m 37s



Application: FPU system

$N=12$. Regular motion on 6d torus. Final time $t=10^8$.

CPU times \approx

8 h

22,5 h

38 h

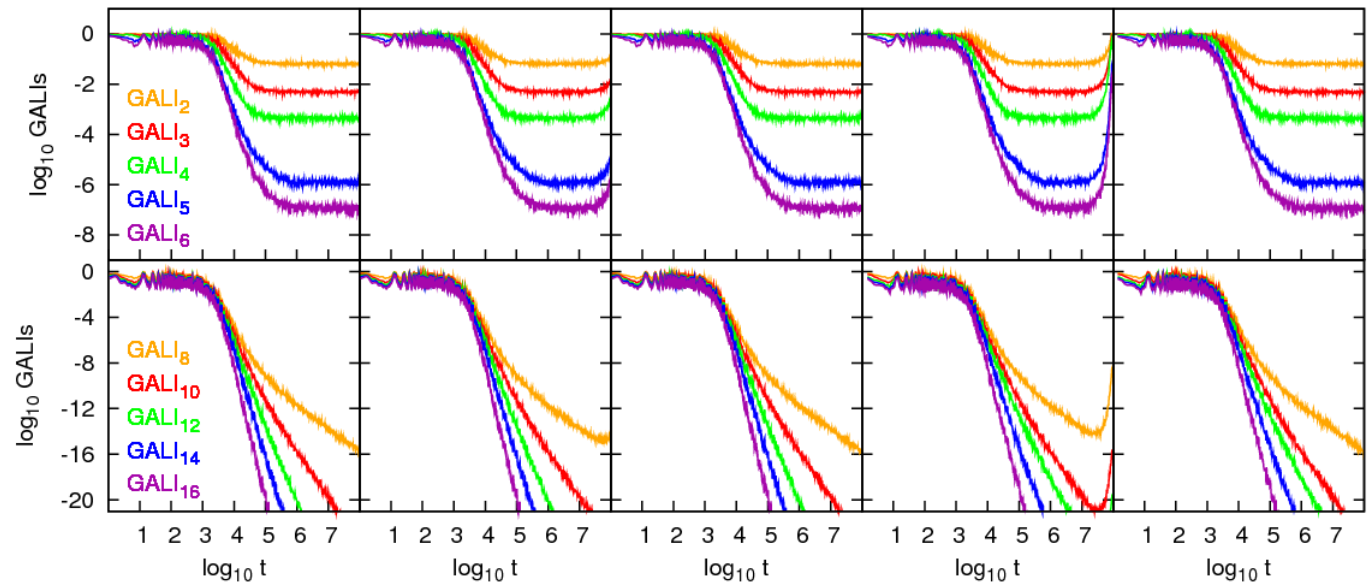
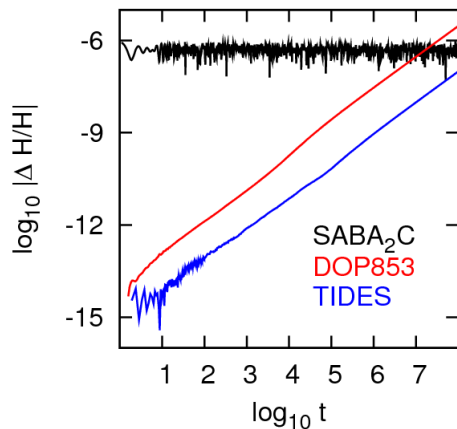
TM, $\tau=0.1$

DOP853, $\delta=10^{-10}$

DOP853, $\delta=10^{-12}$

TIDES, $\delta=10^{-10}$

TIDES, $\delta=10^{-12}$



Conclusions I

- **The Smaller ALignment Index (SALI) method a fast, efficient and easy to compute chaos indicator.**
- **Behaviour of the SALI :**
 - ✓ **2D maps: it tends to zero following completely different time rates for regular and chaotic orbits, which allows the distinction between the two cases.**
 - ✓ **Hamiltonian flows and in multidimensional maps: it goes to zero for chaotic orbits, while it tends to a positive value for ordered orbits.**

Conclusions II

- Generalizing the SALI method we define the Generalized Alignment Index of order k ($GALI_k$) as **the volume of the parallelepiped, whose edges are k unit deviation vectors. $GALI_k$ is computed as the product of the singular values of a matrix (SVD algorithm).**
- Behaviour of $GALI_k$:
 - ✓ **Chaotic motion:** it tends exponentially to zero with exponents that involve the values of several Lyapunov exponents.
 - ✓ **Regular motion:** it fluctuates around non-zero values for $2 \leq k \leq s$ and goes to zero for $s < k \leq 2N$ following power-laws, with s being the dimensionality of the torus.

Conclusions III

- **GALI_k indices :**
 - ✓ can **distinguish rapidly and with certainty between regular and chaotic motion**
 - ✓ can be used to characterize **individual orbits** as well as **"chart" chaotic and regular domains** in phase space
 - ✓ are perfectly suited for **studying the global dynamics of multidimensional systems** , as well as **of time-dependent models**
 - ✓ can identify regular **motion on low-dimensional tori**
- **SALI/GALI methods have been successfully applied to a variety of conservative dynamical systems of**
 - ✓ **Celestial Mechanics** (e.g. Széll et al., 2004, MNRAS - Soulis et al., 2008, Cel. Mech. Dyn. Astr. - Voyatzis, 2008, Astron. J. - Libert et al., 2011, MNRAS - Racoveanu, 2014, Astron. Nachr.)
 - ✓ **Galactic Dynamics** (e.g. Capuzzo-Dolcetta et al., 2007, Astroph. J. - Carpintero, 2008, MNRAS - Manos & Athanassoula, 2011, MNRAS - Carpintero et al., 2014, MNRAS)
 - ✓ **Nuclear Physics** (e.g. Macek et al., 2007, Phys. Rev. C - Stránský et al., 2007, Phys. Atom. Nucl. - Stránský et al., 2009, Phys. Rev. E - Antonopoulos et al., 2010, PRE)
 - ✓ **Statistical Physics** (e.g. Paleari & Penati, 2008, Lect. Notes Phys. - Manos & Ruffo, 2011, Trans. Theory Stat. Phys. - Christodoulidi & Efthymiopoulos, 2013, Physica D)

Conclusions IV

- **Tangent map (TM) method: Symplectic integrators can be used for the efficient integration of the Hamilton's equations of motion and the variational equations.**
 - ✓ **They reproduce accurately the properties of chaos indicators like the GALIs.**
 - ✓ **These algorithms have better performance than non-symplectic schemes in CPU time requirements. This characteristic is of great importance especially for multidimensional systems.**

Main References I

- **Hamiltonian systems and symplectic maps**
 - ✓ Lieberman A. J. & Lichtenberg M. A. (1992) Regular and Chaotic Dynamics, Springer
 - ✓ Cvitanović P., Artuso R., Dahlqvist P., Mainieri R., Tanner G., Vattay G., Whelan N. & Wirzba A., (2015) Chaos – Classical and Quantum, version 15, <http://chaosbook.org/>
- **Lyapunov exponents**
 - ✓ Oseledec V I (1968) Trans. Moscow Math. Soc. 19 197
 - ✓ Benettin G, Galgani L, Giorgilli A and Strelcyn J-M (1980) Meccanica March 9
 - ✓ Benettin G, Galgani L, Giorgilli A and Strelcyn J-M 1980 Meccanica March 21
 - ✓ Ch.S. (2010) Lect. Notes Phys., 790, 63-135

Main References II

- **SALI**

- ✓ Ch.S. (2001) J. Phys. A, 34, 10029
- ✓ Ch.S., Antonopoulos Ch., Bountis T. C. & Vrahatis M. N. (2003) Prog. Theor. Phys. Supp., 150, 439
- ✓ Ch.S., Antonopoulos Ch., Bountis T. C. & Vrahatis M. N. (2004) J. Phys. A, 37, 6269
- ✓ Bountis T. & Ch.S. (2006) Nucl. Inst Meth. Phys Res. A, 561, 173
- ✓ Boreaux J., Carletti T., Ch.S. & Vittot M. (2012) Com. Nonlin. Sci. Num. Sim., 17, 1725
- ✓ Boreaux J., Carletti T., Ch.S., Papaphilippou Y. & Vittot M. (2012) Int. J. Bif. Chaos, 22, 1250219

- **GALI**

- ✓ Ch.S., Bountis T. C. & Antonopoulos Ch. (2007) Physica D, 231, 30-54
- ✓ Ch.S., Bountis T. C. & Antonopoulos Ch. (2008) Eur. Phys. J. Sp. Top., 165, 5-14
- ✓ Gerlach E., Eggl S. & Ch.S. (2012) Int. J. Bif. Chaos, 22, 1250216
- ✓ Manos T., Ch.S. & Antonopoulos Ch. (2012) Int. J. Bif. Chaos, 22, 1250218
- ✓ Manos T., Bountis T. & Ch.S. (2013) J. Phys. A, 46, 254017

Main References III

- **Reviews on SALI and GALI**
 - ✓ Bountis T.C. & Ch.S. (2012) ‘Complex Hamiltonian Dynamics’, Chapter 5, Springer Series in Synergetics
 - ✓ Ch.S. & Manos T. (2014), submitted (preprint version: [nlin.CD/1412.7401](https://arxiv.org/abs/nlin.CD/1412.7401))
- **TM method**
 - ✓ Ch.S. & Gerlach E. (2010) Phys. Rev. E, 82, 036704
 - ✓ Gerlach E. & Ch.S. (2011) Discr. Cont. Dyn. Sys.-Supp. , 8th AIMS Int. Conference, 475
 - ✓ Gerlach E., Eggl S. & Ch.S. (2012) Int. J. Bif. Chaos, 22, 1250216